TABLE: Summary of the Clinical Features of Subjects with *KCNQ2* Mutations

Case #	Mutation	Sex	Age	Age at Onset, Days	Initial Symptoms	Initial Epileptic Attacks	Initial EEG	Age at Onset of Spasms, Days	Age at Onset of SB Pattern, Days	Response to Therapy	Other Drugs Used, but Ineffective	Development	Neurological Examination	Involuntary Movement
1469	c.1010C>G (p.A337G) de novo	M	7 years	7	Vomiting	7 days, tonic seizure	SB	—	22	Seizure free and SB on EEG, disappeared after high-dose PB, CPS since age 5 years	B6, ZNS	No meaningful words, able to crawl, stand with support	Severe MR, no pyramidal signs	No
1654	c.341C>T (p.T114I) de novo	F	7 years	0	Tremor of the upper extremities	2 days, generalized convulsion with cyanosis	SB	—	2	Seizure free after ZNS, CPS since age 5 years	B6, CZP, PHT	DQ 10, bed-ridden, smiling	Profound MR, spastic quadriplegia	No
1754	c.794C>T (p.A265V) de novo	M	3 months	1	Apneic spell	1 days, tonic spasms with right opsoclonuslike movement	SB	1	2	Intractable	B6, ZNS, VPA, CZP, CBZ	Delayed, no eye pursuit	Unknown	Myoclonus at the bilateral upper extremities

B6 = vitamin B6; CBZ = carbamazepine; CPS = complex partial seizures; CZP = clonazepam; DQ = developmental quotient; EEG = electroencephalogram; MR = mental retardation; PB = phenobarbital; PHT = phenytoin; SB = suppression–burst; VPA = valproic acid; ZNS = zonisamide.

patients with OS, we found 3 missense mutations in *KCNQ2* (25%): c.341C>T (p.T114I), c.1010C>G (p.A337G), and c.794C>T (p.A265V) in 3 patients. All 3 patients showed initial seizures early in the neonatal period and a characteristic suppression–burst pattern on EEG, leading to diagnosis as OS (Table). Seizures were temporarily well controlled in 2 patients. Consistent with Weckhuysen's report, in which 6 of 8 mutations arose de novo, the 3 mutations in our series are de novo changes. Thus, it is likely that de novo *KCNQ2* mutations are among the common causes of early onset epileptic encephalopathies, including OS. *KCNQ2* mutations have been shown to cause benign familial neonatal seizures, which is distinct from OS.[2,3] We unexpectedly found *KCNQ2* mutations by whole exome sequencing. Exome sequencing using familial trios (patients and their parents) can identify de novo mutations.[4] Novel associations between unexpected gene mutations and early onset epileptic encephalopathies may be validated by such new technologies.

Acknowledgment

Supported by a research grant from the Ministry of Health, Labor, and Welfare, Japan (H.S., M.K., N.Mi., N.Ma.), a Grant-in-Aid for Scientific Research from the Japan Society for the Promotion of Science (H.S., M.K., N.Mi., N.Ma.), a research grant from the Japan Science and Technology Agency (N.Ma.), and the Strategic Research Program for Brain Sciences (a Grant-in-Aid for Scientific Research on Innovative Areas, Foundation of Synapse and Neurocircuit Pathology; N.Ma.).

Potential Conflicts of Interest

Nothing to report.

[1]Department of Human Genetics, Yokohama City University Graduate School of Medicine, Yokohama, [2]Department of Pediatrics, Yamagata University Faculty of Medicine, Yamagata, [3]Department of Neurology, Tokyo Metropolitan Children's Medical Center, Fuchu, and [4]Department of Pediatrics, Fukuoka University Faculty of Medicine, Fukuoka, Japan

References

1. Weckhuysen S, Mandelstam S, Suls A, et al. KCNQ2 encephalopathy: emerging phenotype of a neonatal epileptic encephalopathy. Ann Neurol 2012;71:15–25.
2. Singh NA, Charlier C, Stauffer D, et al. A novel potassium channel gene, KCNQ2, is mutated in an inherited epilepsy of newborns. Nat Genet 1998;18:25–29.

3. Biervert C, Schroeder BC, Kubisch C, et al. A potassium channel mutation in neonatal human epilepsy. Science 1998;279: 403–406.

4. Vissers LE, de Ligt J, Gilissen C, et al. A de novo paradigm for mental retardation. Nat Genet 2010;42:1109–1112.

DOI: 10.1002/ana.23620

Brain Death in Children: Why Does It Have to Be So Complicated?

Thomas Nakagawa, MD,[1] Stephen Ashwal, MD,[2] Mudit Mathur, MD,[3] and Mohan Mysore, MD[4]

The authors appreciate the editorial comments by Wijdicks and Smith[1] and would like to address concerns about why the diagnosis of brain death in pediatric patients has to be "so complicated."

This revised clinical guideline focused specifically on determining brain death and deliberately excluded issues related to ethical concerns and organ donation. Failure to mention the Child Neurology Society (CNS) as the third sponsoring society of this guideline is a major oversight of the editorial.[1] CNS provided significant review by Practice Committee members and the society's Executive Board.[2] The quality of evidence provided in this guideline was equivalent to, if not more comprehensive than, the revised American Academy of Neurology (AAN) guideline, which reported only class III or IV evidence for 4 of 5 questions posed.[3] We used the GRADE system to develop a consensus guideline because no class I or II studies to determine pediatric brain death exist.[2] Interestingly, the AAN is currently revising guideline development for practicing neurologists to use a modification of the GRADE system.

A wide range of clinical entities can result in brain death in newborns, children, and adolescents. The guideline, the checklist, and Table 3 clearly state that all reversible conditions should be excluded prior to the first brain death examination. However, some uncertainty in the newborn period still exists leading to age-based observation periods. These consensus based recommendations reflect extensive clinical experience across several pediatric disciplines. Additionally, provisions for pediatric trauma patients and neonates were included. Virtually every committee member has cared for acutely injured children who met examination criteria for brain death within the initial 24 hours. Some recovered brain function although most did not which is why 2 examinations over defined time periods is recommended. The recommended time periods are consensus based rather than arbitrary time periods. Neurologic examination findings remaining unchanged and consistent with brain death throughout the observation period was one of the recommended criteria for determining brain death in the 1987 guidelines. The committee retained this recommendation in the current update. We agree that apparent neurologic improvements reported in anecdotal cases are due to diagnostic errors when critically examined; this is precisely the reason why a change in findings between examinations implies the neurological process is potentially reversible, precluding the diagnosis of brain death.

The revised guideline repeatedly states that brain death is a clinical diagnosis, and factors influencing the neurologic examination must be corrected before initiating brain death evaluation and apnea testing. Ancillary studies do not trump the neurological examination, and we clearly state that ancillary studies should not be viewed as a substitute for the neurologic examination. However, situations exist where ancillary studies are helpful to determine death. The revised guideline and checklist have simplified and clarified many previous sources of confusion. Additionally, the checklist will help standardize determination and documentation of brain death in children.[4]

Prolonging declaration of death does not appear to be a major concern in children—perhaps differing from the experience in adults. Families appreciate the added certainty conferred by the second examination. Patients in children's hospitals rely on assessments by pediatric specialists who understand the unique needs of children and their families. The approach to caring for children is very different and likely more family centered. These issues are further addressed in the full guideline and we encourage readers to review the entire document published in Critical Care Medicine and Pediatrics.[2,5]

Declaring brain death in children is complicated and should be undertaken by physicians who are adequately trained in the complexities involved in this important determination. We agree more research is needed to address some of the other issues raised in the editorial, and we again thank Drs Wijdicks and Smith for their opinion.

Potential Conflicts of Interest

Nothing to report.

[1]Departments of Anesthesiology (Section on Pediatric Critical Care) and Pediatrics, Wake Forest School of Medicine, Winston-Salem, NC, [2]Department of Pediatrics (Division of Child Neurology) and [3]Division of Pediatric Critical Care, Loma Linda University School of Medicine, Loma Linda, CA, and [4]Department of Pediatrics, University of Nebraska College of Medicine, Omaha, NE

References

1. Wijdicks EF, Smith WS. Brain death in children: why does it have to be so complicated? Ann Neurol 2012;71:442–443.

2. Nakagawa TA, Ashwal S, Mathur M, et al. Guidelines for the determination of brain death in infants and children: an update of the 1987 Task Force recommendations. Crit Care Med 2011;39:2139–2155.

3. Wijdicks EF, Varelas PN, Gronseth GS, et al. Evidence-based guideline update: determining brain death in adults: report of the Quality Standards Subcommittee of the American Academy of Neurology. Neurology 2010;74:1911–1918.

4. Fackler J, Goldstein B. Pediatric brain death. Crit Care Med 2011; 39;2197–2198.

5. Clinical report - Guidelines for the Determination of Brain Death in Infants and Children. An Update of the 1987 Task Force Recommendations. Nakagawa TA, Ashwal, SA, Mathur M, Mysore M., and the Committee for Brain Death in Infants and Children. Pediatrics. 2011;128:3 e720-e740. doi: 10.1542/peds.2011-1511.

DOI: 10.1002/ana.23623

nature genetics

Mutations affecting components of the SWI/SNF complex cause Coffin-Siris syndrome

Yoshinori Tsurusaki[1], Nobuhiko Okamoto[2], Hirofumi Ohashi[3], Tomoki Kosho[4], Yoko Imai[5], Yumiko Hibi-Ko[5], Tadashi Kaname[6], Kenji Naritomi[6], Hiroshi Kawame[7,8], Keiko Wakui[4], Yoshimitsu Fukushima[4], Tomomi Homma[9], Mitsuhiro Kato[10], Yoko Hiraki[11], Takanori Yamagata[12], Shoji Yano[13], Seiji Mizuno[14], Satoru Sakazume[15], Takuma Ishii[15,16], Toshiro Nagai[15], Masaaki Shiina[17], Kazuhiro Ogata[17], Tohru Ohta[18], Norio Niikawa[18], Satoko Miyatake[1], Ippei Okada[1], Takeshi Mizuguchi[1], Hiroshi Doi[1], Hirotomo Saitsu[1], Noriko Miyake[1] & Naomichi Matsumoto[1]

By exome sequencing, we found *de novo SMARCB1* mutations in two of five individuals with typical Coffin-Siris syndrome (CSS), a rare autosomal dominant anomaly syndrome. As *SMARCB1* encodes a subunit of the SWItch/Sucrose NonFermenting (SWI/SNF) complex, we screened 15 other genes encoding subunits of this complex in 23 individuals with CSS. Twenty affected individuals (87%) each had a germline mutation in one of six SWI/SNF subunit genes, including *SMARCB1*, *SMARCA4*, *SMARCA2*, *SMARCE1*, *ARID1A* and *ARID1B*.

Chromatin remodeling factors regulate the gene accessibility and expression by dynamic alteration of chromatin structure. SWI/SNF complexes have important roles in lineage specification, maintenance of stem cell pluripotency and tumorigenesis[1–5]. These complexes are composed of evolutionarily conserved core subunits and variant subunits. Brahma-associated factor (BAF) and Polybromo BAF (PBAF) complexes constitute two major subclasses[1–5]. It has been suggested that the BAF complex is similar to the yeast SWI/SNF complex and that the PBAF complex is more like the chromatin remodelling complex (RSC) in yeast, which is required for cell cycle progression through mitosis[6]. However, several subunits that are common to both BAF and PBAF complexes are predicted to be related to the regulation of lineage- and tissue-specific gene expression[2].

Coffin-Siris syndrome (MIM 135900) is a rare congenital anomaly syndrome characterized by growth deficiency, intellectual disability, microcephaly, coarse facial features and hypoplastic nail of the fifth finger and/or toe (**Fig. 1** and **Supplementary Table 1**)[7]. The majority of affected individuals represent sporadic cases, which is compatible with an autosomal dominant inheritance mechanism. The genetic cause for this syndrome has not been elucidated.

To identify the genetic basis of CSS, we performed whole-exome sequencing of five typical affected individuals (**Supplementary Methods**). Taking into account our model that assumes that an abnormality in a causal gene would be shared in two or more subjects, 51 variants were identified as candidates (**Supplementary Table 2**). All the variants were also examined by Sanger sequencing of PCR products amplified using genomic DNA from the five affected individuals and their parents. Nine variants were found to be false positives, 40 were inherited from either the father or mother, and 2 *de novo* heterozygous mutations of *SMARCB1* were found in 2 affected individuals (c.1130G>A (p.Arg377His) and c.1091_1093del AGA (p.Lys364del)) (**Table 1**, **Supplementary Fig. 1** and **Supplementary Methods**). Two *de novo* coding-sequence mutations occurring within a specific gene is an extremely unlikely event[8], supporting the idea that *SMARCB1* is a causative gene in CSS. Next, we screened *SMARCB1* in 23 individuals with CSS by high-resolution melting analysis[9] and identified the mutation encoding the p.Lys364del alteration in two additional individuals, including one of Arab descent (subject 22) (**Table 1** and **Supplementary Fig. 1**). As the mutation detection rate was relatively low (4 of 23, only 17.4%), we screened 15 additional genes encoding other SWI/SNF subunits (**Supplementary Table 3**). Unexpectedly, four other subunits, *SMARCA4* (also known as *BRG1*), *SMARCE1*, *ARID1A* and *ARID1B* were also found to be mutated (**Table 1** and **Supplementary Figs. 2–5**). In subject 10, a, c.2144C>T mutation in *ARID1B* (encoding p.Pro715Leu) was found in addition to the c.5632delG mutation in *ARID1B*. RT-PCR products that were amplified from total RNA from this subject's lymphoblastoid cells were cloned into the pCR4-TOPO vector. The two mutations were present on different alleles, according to sequencing of clones containing each allele (data not shown). As the c.5632delG mutation is

[1]Department of Human Genetics, Yokohama City University Graduate School of Medicine, Yokohama, Japan. [2]Division of Medical Genetics, Osaka Medical Center and Research Institute for Maternal and Child Health, Izumi, Japan. [3]Division of Medical Genetics, Saitama Children's Medical Center, Iwatsuki, Japan. [4]Department of Medical Genetics, Shinshu University School of Medicine, Matsumoto, Japan. [5]Division of Pediatrics, Japanese Red Cross Medical Center, Tokyo, Japan. [6]Department of Medical Genetics, University of the Ryukyus Faculty of Medicine, Okinawa, Japan. [7]Department of Genetic Counseling, Graduate School of Humanities and Sciences, Ochanomizu University, Tokyo, Japan. [8]Division of Medical Genetics, Nagano Children's Hospital, Azumino, Japan. [9]Division of Pediatrics, Yamagata Prefectural and Sakata Municipal Hospital Organization, Nihonkai General Hospital, Sakata, Japan. [10]Department of Pediatrics, Yamagata University Faculty of Medicine, Yamagata, Japan. [11]Hiroshima Municipal Center for Child Health and Development, Hiroshima, Japan. [12]Department of Pediatrics, Jichi Medical University, Tochigi, Japan. [13]Genetics Division, Department of Pediatrics, Los Angeles County and University of Southern California Medical Center, Keck School of Medicine, University of Southern California, Los Angeles, California, USA. [14]Department of Pediatrics, Central Hospital, Aichi Human Service Center, Kasugai, Japan. [15]Department of Pediatrics, Koshigaya Hospital, Dokkyo University School of Medicine, Koshigaya, Japan. [16]Nakagawa-No-Sato, Hospital for the Disabled, Saitama, Japan. [17]Department of Biochemistry, Yokohama City University Graduate School of Medicine, Yokohama, Japan. [18]Research Institute of Personalized Health Sciences, Health Sciences University of Hokkaido, Ishikari-Tobetsu, Japan. Correspondence should be addressed to N. Matsumoto (naomat@yokohama-cu.ac.jp) or N. Miyake (nmiyake@yokohama-cu.ac.jp).

Received 29 September 2011; accepted 10 February 2012; published online 18 March 2012; doi:10.1038/ng.2219

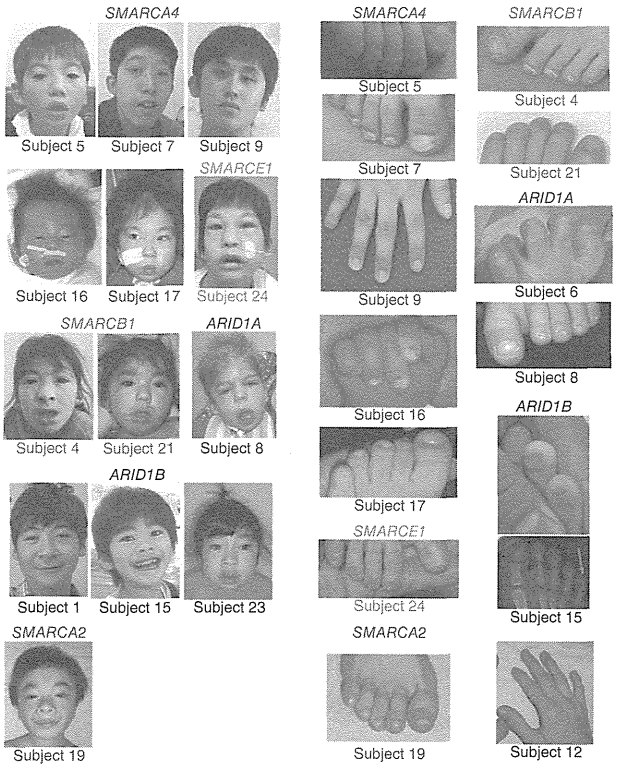

Figure 1 Photographs of individuals with Coffin-Siris syndrome. The faces (left) and hypoplastic-to-absent nail of the fifth finger or toe (right) of affected individuals are shown with the color-coded names of the corresponding mutated genes. The green arrow indicates the absence of the distal phalanx in the fifth toe. No obvious hypoplastic nails were observed in subjects 12 or 19. Consent for all the photographs was obtained from the families of the affected individuals.

very likely to be deleterious (as it results in a truncated protein), the c.2144C>T mutation is likely to be a rare polymorphism. Of note, subject 12, who presented an atypical facial appearance and indistinct hypoplastic nails, had two interstitial deletions at 6q25.3–q27 involving *ARID1B*, as detected by a SNP array (**Supplementary Fig. 6** and **Supplementary Methods**). Furthermore, subject 14 was found to have an interstitial deletion of *SMARCA2* by a SNP array (**Supplementary Fig. 7** and **Supplementary Methods**). No other copy-number changes involving genes encoding SWI/SNF complex components were found in subjects 2, 14 or 18 by array analysis. The overall mutation detection rate was 87%. In total, 20 of the 23 subjects had a mutation affecting one of the six SWI/SNF subunits.

Mutations in CSS were identified in the BAF-specific subunits *ARID1A* and *ARID1B* but not in PBAF-specific subunits (*BRD7*, *ARID2* and *PBRM1*) (**Supplementary Table 3**). In addition, mutations were identified in *SMARCA4* (*BRG1*) as well as in *SMARCA2* (*BRM*) (**Supplementary Table 3**). The BRG1 and BRM proteins are mutually exclusive catalytic ATP subunits in mammalian SWI/SNF complexes. Of note, the majority of heterozygous *Smarca4*-null mice survive with susceptibility to neoplasia, with a minority dying after birth because of exencephaly, whereas homozygous *Smarca2*-null mice are viable and fertile[4]. In *Smarca2*-null mice, Brg1 is upregulated, suggesting that Brg1 can functionally replace Brm in mice[10]. However, in humans, abnormalities in both *SMARCA4* and *SMARCA2* are found in CSS, indicating that the in-frame partial deletion of the gene encoding BRM in subject 19 has a specific mutational effect different from that of simple inactivation in mice. These data support the idea that abnormalities in the BRG1-BAF and BRM-BAF complexes can cause the abnormal neurological development in CSS.

All the mutated genes found in CSS, except for *SMARCE1*, have been reported to be associated with tumorigenesis[1,2]. Among the 23 subjects with CSS, only subject 3 with an *ARID1A* mutation presented with hepatoblastoma. To our knowledge, haploinsufficiency and/or homozygous inactivation of *ARID1A* have been found in several types of cancer but not in hepatoblastoma. Malignancies were not detected in any of the other subjects with CSS examined here. It remains to be seen whether malignancies are robustly associated with CSS.

Given the fact that all the mutations in *ARID1A* and *ARID1B* in CSS were predicted to cause protein truncation, we proposed that haploinsufficiency of these two genes must be able to cause CSS. cDNA analysis of lymphoblastoid cell lines from subjects 1, 6 and 23 indicated that the mutated transcripts were subject to nonsense-mediated mRNA decay (**Supplementary Fig. 8**). In subject 10, the *ARID1B* mutation associated with the creation of a premature stop codon in the last exon did not result in nonsense-mediated mRNA decay as expected (**Supplementary Fig. 8**).

In regard to the other mutated genes, germline heterozygous truncation mutations in *SMARCB1* and *SMARCA4* have been reported

Table 1 Mutations in individuals with Coffin-Siris syndrome

Subject ID	Gene	Mutation	Alteration	Type	Control allele frequency[a]
4	*SMARCB1*	c.1091_1093del AGA	p.Lys364del	*De novo*	0/502
11	*SMARCB1*	c.1130G>A	p.Arg377His	*De novo*	0/500
21	*SMARCB1*	c.1091_1093del AGA	p.Lys364del	NC	0/502
22	*SMARCB1*	c.1091_1093del AGA	p.Lys364del	NC	0/502
9	*SMARCA4*	c.1636_1638del AAG	p.Lys546del	*De novo*	0/350
7	*SMARCA4*	c.2576C>T	p.Thr859Met	*De novo*	0/368
5	*SMARCA4*	c.2653C>T	p.Arg885Cys	*De novo*	0/368
16	*SMARCA4*	c.2761C>T	p.Leu921Phe	*De novo*	0/368
25	*SMARCA4*	c.3032T>C	p.Met1011Thr	NC	0/372
17	*SMARCA4*	c.3469C>G	p.Arg1157Gly	*De novo*	0/368
19	*SMARCA2*	Partial deletion		*De novo*	–
24	*SMARCE1*	c.218A>G	p.Tyr73Cys	*De novo*	0/368
3	*ARID1A*	c.31_56del	p.Ser11Alafs*91	NC	0/330
6	*ARID1A*	c.2758C>T	p.Gln920*	NC	0/376
8	*ARID1A*	c.4003C>T	p.Arg1335*	*De novo*	–
1	*ARID1B*	c.1678_1688del	p.Ile560Glyfs*89	*De novo*	–
15	*ARID1B*	c.1903C>T	p.Gln635*	*De novo*	–
23	*ARID1B*	c.3304C>T	p.Arg1102*	*De novo*	–
10	*ARID1B*	c.2144C>T	p.Pro715Leu	NC	0/368
10	*ARID1B*	c.5632del G	p.Asp1878Metfs*96	NC	0/374
12	*ARID1B*	Microdeletion		NC	–

NC, not confirmed because parental samples were unavailable.
[a]The numbers indicate the observed allele frequency (alleles harboring the change/total tested alleles) in Japanese controls. None of the mutations was found in dbSNP132, the 1000 Genomes database or the National Heart, Lung, and Blood Institute (NHLBI) GO exomesequencing project database. –, not tested.

in individuals with rhabdoid tumor predisposition syndromes 1 (RTPS1; MIM 609322) and 2 (RTPS2; MIM 613325)[11,12], and various types of *SMARCB1* mutations (missense, in-frame deletion, nonsense and splice site) have been found in the germline of individuals with familial and sporadic schwannomatosis (MIM 162091)[13,14]. Furthermore, mice with heterozygous knockout of *Smarca4* or *Smarcb1* were prone to tumor development[2]. All the mutations in *SMARCA4* and *SMARCB1* in individuals with CSS were non-truncating (either missense or in-frame deletions), implying that they exert gain-of-function or dominant-negative effects (excluding haploinsufficiency as a cause). It is noteworthy that comparable germline mutations in *SMARCB1* have such different phenotypic consequences in their association with the phenotypes of CSS and schwannomatosis. The *SMARCB1* mutations in CSS and those in schwannomatosis are indeed different according to the Human Gene Mutation Database. With regard to the *SMARCA2* interstitial deletion in CSS, the change maintained the coding sequence reading frame but removed exons 20–27 that encode the HELICc domain. RT-PCR analysis confirmed the deletion of exons 20–27 at the cDNA level (**Supplementary Fig. 7**). These data suggest the importance of the HELICc domain in the SMARCA2 protein.

The various types of mutations in the genes encoding different SWI/SNF components resulted in similar CSS phenotypes. This suggests that the SWI/SNF complexes coordinately regulate chromatin structure and gene expression. This is the first report, to our knowledge, of germline mutations in SWI/SNF complex genes associated with a multiple congenital anomaly syndrome, highlighting new biological aspects of SWI/SNF complexes in humans. Similarly, genes encoding SNF2-related proteins, which are implicated as chromatin remodeling factors outside of SWI/SNF complexes, are mutated in different syndromes, including in α-thalassaemia/mental retardation syndrome X-linked (ATRX; *ATRX* mutations) and in coloboma, heart defect, atresia choanae, retarded growth and development, genital abnormality and ear abnormality (CHARGE) syndrome (*CHD7* haploinsufficiency)[3]. We expect that more mutations affecting chromatin remodeling factors will be found in different human diseases.

URLs. Human Gene Mutation Database, https://portal.biobase-international.com/cgi-bin/portal/login.cgi.

Note: Supplementary information is available on the Nature Genetics website.

ACKNOWLEDGMENTS

We thank all the family members for participating in this study. This work was supported by research grants from the Ministry of Health, Labour and Welfare (to N. Miyake, H.S. and N. Matsumoto), the Japan Science and Technology Agency (to N. Matsumoto), the Strategic Research Program for Brain Sciences (to N. Matsumoto), the Japan Epilepsy Research Foundation (to H.S.) and the Takeda Science Foundation (to N. Matsumoto and N. Miyake). This study was also funded by a Grant-in-Aid for Scientific Research on Innovative Areas (Foundation of Synapse and Neurocircuit Pathology) from the Ministry of Education, Culture, Sports, Science and Technology of Japan (to N. Matsumoto), a Grant-in-Aid for Scientific Research from the Japan Society for the Promotion of Science (to N. Matsumoto), a Grant-in-Aid for Young Scientists from the Japan Society for the Promotion of Science (to N. Miyake and H.S.) and a Grant for 2011 Strategic Research Promotion of Yokohama City University (to N. Matsumoto). This study was performed at the Advanced Medical Research Center at Yokohama City University. Informed consent was obtained from all the families of affected individuals. The Institutional Review Board of Yokohama City University approved this study.

AUTHOR CONTRIBUTIONS

Y.T., S. Miyatake, I.O., H.D., H.S. and N. Miyake performed exome sequencing and Sanger sequencing. Y.T., M.S., K.O., I.O., T.M., H.D., H.S. and N. Miyake performed data management and analysis. N.O., H.O., T. Kosho, Y.I., Y.H.-K., T. Kaname, K.N., H.K., K.W., Y.F., T.H., M.K., Y.H., T.Y., S.Y., S. Mizuno, S.S., T.I., T.N., T.O. and N.N. provided clinical materials after careful evaluation. Y.T., N. Miyake and N. Matsumoto wrote the manuscript. N. Matsumoto designed and oversaw all aspects of the study.

COMPETING FINANCIAL INTERESTS

The authors declare no competing financial interests.

Published online at http://www.nature.com/naturegenetics/.
Reprints and permissions information is available online at http://www.nature.com/reprints/index.html.

1. Reisman, D., Glaros, S. & Thompson, E.A. *Oncogene* **28**, 1653–1668 (2009).
2. Wilson, B.G. & Roberts, C.W. *Nat. Rev. Cancer* **11**, 481–492 (2011).
3. Clapier, C.R. & Cairns, B.R. *Annu. Rev. Biochem.* **78**, 273–304 (2009).
4. Bultman, S. *et al. Mol. Cell* **6**, 1287–1295 (2000).
5. Hargreaves, D.C. & Crabtree, G.R. *Cell Res.* **21**, 396–420 (2011).
6. Xue, Y. *et al. Proc. Natl. Acad. Sci. USA* **97**, 13015–13020 (2000).
7. Coffin, G.S. & Siris, E. *Am. J. Dis. Child.* **119**, 433–439 (1970).
8. Bamshad, M.J. *et al. Nat. Rev. Genet.* **12**, 745–755 (2011).
9. Wittwer, C.T., Reed, G.H., Gundry, C.N., Vandersteen, J.G. & Pryor, R.J. *Clin. Chem.* **49**, 853–860 (2003).
10. Reyes, J.C. *et al. EMBO J.* **17**, 6979–6991 (1998).
11. Schneppenheim, R. *et al. Am. J. Hum. Genet.* **86**, 279–284 (2010).
12. Taylor, M.D. *et al. Am. J. Hum. Genet.* **66**, 1403–1406 (2000).
13. Boyd, C. *et al. Clin. Genet.* **74**, 358–366 (2008).
14. Hadfield, K.D. *et al. J. Med. Genet.* **45**, 332–339 (2008).

Hum Genet (2012) 131:591–599
DOI 10.1007/s00439-011-1105-7

ORIGINAL INVESTIGATION

Rapid detection of gene mutations responsible for non-syndromic aortic aneurysm and dissection using two different methods: resequencing microarray technology and next-generation sequencing

Haruya Sakai · Shinichi Suzuki · Takeshi Mizuguchi · Kiyotaka Imoto · Yuki Yamashita · Hiroshi Doi · Masakazu Kikuchi · Yoshinori Tsurusaki · Hirotomo Saitsu · Noriko Miyake · Munetaka Masuda · Naomichi Matsumoto

Received: 14 July 2011 / Accepted: 4 October 2011 / Published online: 15 October 2011

Abstract Aortic aneurysm and/or dissection (AAD) is a life-threatening condition, and several syndromes are known to be related to AAD. In this study, two new technologies, resequencing array technology (ResAT) and next-generation sequencing (NGS), were used to analyze eight genes associated with syndromic AAD in 70 patients with non-syndromic AAD. Eighteen sequence variants were detected using both ResAT and NGS. In addition one of these sequence variants was detected by ResAT only and two additional variants by NGS only. Three of the 18 variants are likely to be pathogenic (in 4.3% of AAD patients and in 8.6% of a subset of patients with thoracic AAD), highlighting the importance of genetic analysis in non-syndromic AAD. ResAT and NGS similarly detected most, but not all, of the variants. Resequencing array technology was a rapid and efficient method for detecting most nucleotide substitutions, but was unable to detect short insertions/deletions, and it is impractical to update custom arrays frequently. Next-generation sequencing was able to detect almost all types of mutation, but requires improved informatics methods.

Electronic supplementary material The online version of this article (doi:10.1007/s00439-011-1105-7) contains supplementary material, which is available to authorized users.

H. Sakai · T. Mizuguchi · Y. Yamashita · H. Doi · M. Kikuchi · Y. Tsurusaki · H. Saitsu · N. Miyake · N. Matsumoto (✉)
Department of Human Genetics, Yokohama City University Graduate School of Medicine, 3-9 Fukuura, Kanazawa-ku, Yokohama 236-0004, Japan
e-mail: naomat@yokohama-cu.ac.jp

S. Suzuki · M. Masuda
Department of Surgery, Yokohama City University Graduate School of Medicine, Yokohama, Japan

K. Imoto
Cardiovascular Center, Yokohama City University Medical Center, 4-57 Urafune, Minami-ku, Yokohama 232-0024, Japan

Introduction

Aortic aneurysm and/or dissection (AAD) is a life-threatening condition. As significant symptoms do not usually appear before the rupture of the AAD, which can be lethal, it is often difficult to prevent death from AAD. Timely cardiovascular surgery may prevent AAD rupture and save the patient's life. Approximately 20% of patients with thoracic aortic disease have a family history of the disease, which is typically inherited in an autosomal dominant manner with decreased penetrance and variable expressivity (Wang et al. 2010). Therefore, if a causative mutation is detected in a patient, it is worth checking for the mutation in their asymptomatic family members to prevent future aortic events by medical and/or surgical intervention. Several genes are known to be associated with syndromes presenting with hereditary AAD and vascular disruption: *FBN1* (Dietz et al. 1991; Lee et al. 1991a), *TGFBR2* (Mizuguchi et al. 2004), *TGFBR1* (Loeys et al. 2005), *MYH11* (Zhu et al. 2006), *ACTA2* (Guo et al. 2007), *COL3A1* (Superti-Furga et al. 1988), *PLOD1* (Hautala et al. 1993), and *SLC2A10* (Coucke et al. 2006) (Table 1). Most AAD patients who have been surgically treated are not affected by these syndromes. However, the contribution of these genes to non-syndromic AAD has not been thoroughly investigated. A comprehensive study of these genes by conventional Sanger sequencing is a huge and expensive undertaking. Even high-resolution melting methods and denaturing high performance liquid chromatography require the amplification of at least 210 exons from these eight genes (Table 1). Therefore, it has been unrealistic for most laboratories to analyze these genes in multiple samples.

Table 1 Overview of genes associated with AAD analyzed in this study

Gene	GenBank accession no.	Disorder	Type	Exon (CDE)	ORF (bp)	Amplicon
FBN1	NM_000138	MFS, SGS, TAAD	AD	66 (65)	8,616	39
TGFBR2	NM_001024847	MFS2, LDS, SGS, TAAD	AD	8 (8)	1,779	8
TGFBR1	NM_004612	MFS2, LDS, SGS, TAAD	AD	9 (9)	1,512	7
COL3A1	NM_000090	EDS type IV	AD	51 (51)	4,401	16
PLOD1	NM_000302	EDS type VI	AR	19 (19)	2,184	13
MYH11	NM_001040113	TAAD	AD	43 (41)	5,838	30
SLC2A10	NM_030777	ATS	AR	5 (5)	1,626	5
ACTA2	NM_001613	TAAD	AD	9 (8)	1,134	6

CDE coding exon, *ORF* open reading frame, *MFS* Marfan syndrome, *MFS2* Marfan syndrome type II, *LDS* Loeys–Dietz syndrome, *SGS* Shprintzen–Goldberg syndrome, *TAAD* thoracic aortic aneurysm and dissection, *EDS* Ehlers–Danlos syndrome, *ATS* arterial tortuosity syndrome, *AD* autosomal dominant, *AR* autosomal recessive

Resequencing array technology (ResAT) enables the investigation of multiple genes on one chip. This technology has been used for multiple-gene analysis in childhood hearing loss (Kothiyal et al. 2010), breast-ovarian cancer syndrome (Schroeder et al. 2010), dilated cardiomyopathy (Zimmerman et al. 2010), X-linked intellectual disability (Jensen et al. 2011), familial hypercholesterolemia (Chiou et al. 2011), and hypertrophic cardiomyopathy (Fokstuen et al. 2011). Different research groups have shown ResAT to be a highly efficient, relatively accurate, cost-effective, and rapid method. However, several drawbacks have been pointed out, including its insensitivity in detecting nucleotide insertions/deletions (indels) and nucleotide changes in GC-rich regions and repeat sequences.

Next-generation sequencing (NGS) is now regarded as the most powerful technology for detecting mutations (Ng et al. 2010; Tsurusaki et al. 2011). This platform is advantageous in finding almost all types of mutations including small indel mutations. The high throughput and multiplexing of NGS allows multiple genes to be sequenced in many samples in a single run (Farias-Hesson et al. 2010; Gabriel et al. 2009).

In this study, we analyzed the eight AAD-associated genes (*FBN1*, *TGFBR2*, *TGFBR1*, *COL3A1*, *PLOD1*, *MYH11*, *SLC2A10*, and *ACTA2*) in 70 patients with non-syndromic AAD by two methods: ResAT (all eight genes on one chip) and multiplex NGS. We describe here a comparison of the results.

Materials and methods

Patients

Seventy Japanese patients, who had surgery for AAD, were recruited from Yokohama City University Hospital and Yokohama City University Medical Center. The patients' clinical information is summarized in Table 2. Thoracic AAD involves the aorta above the diaphragm and abdominal AAD is located along the portion of the aorta passing through the abdomen. None of the patients in this study had any clinical test results supporting a diagnosis of syndromic AAD. Experimental protocols were approved by the Institutional Review Board of Yokohama City University School of Medicine. Informed consent for genetic analysis was obtained from the patients. DNA was extracted from peripheral blood leukocytes using a QuickGene-610L kit (Fujifilm, Tokyo, Japan).

Table 2 Clinical information of AAD patients

Clinical data	Number of patients (%)
Thoracic AAD[a]	35 (50.0)
Abdominal AAD[a]	30 (42.9)
Thoracic and abdominal AAD[a]	5 (7.1)
Age (years) (mean ± SD)	67.3 ± 10.2 (range 39–83)
Age (years) (median)	68.5
<50 years old	4 (5.7)
50–54 years old	5 (7.1)
55–59 years old	8 (11.4)
≥60 years old	53 (75.7)
Male	53 (75.7)
Female	17 (24.3)
Diabetes	9 (12.9)
Hyperlipidemia	32 (45.7)
Hypertension	54 (77.1)
Current smoker	15 (21.4)
Past smoker	30 (42.9)
Never smoked	23 (32.9)

[a] Including current and past operations

Array design

Eight genes (*FBN1*, *TGFBR2*, *TGFBR1*, *COL3A1*, *PLOD1*, *MYH11*, *SLC2A10* and *ACTA2*) (Table 1) associated with AAD were selected for one custom chip (Affymetrix, Santa Clara, CA). All coding exons as well as 29 bp of sequence from each intron (21 bp on the 5′-side and 8 bp on the 3′-side of each exon) were analyzed. Repetitive sequences and intragenic low complexity regions larger than 25 bp were excluded from the chip. A total of 33,116 bp from the eight genes could be sequenced using this chip.

PCR amplification, purification, hybridization, scanning, and data analysis

The targeted regions were amplified as 124 fragments by PCR (ranging from 965 to 2,999 bp) using Blend Taq Plus (TOYOBO, Osaka, Japan) or KOD FX (TOYOBO) and genomic DNA as a template in a 20 μL volume. The PCR conditions were: denaturing at 94°C, 35 cycles of 94°C for 30 s, 62°C for 30 s, and 72°C for 3 min, and a final extension at 72°C for 7 min. The DNA concentration of the amplicons was determined using a Quant-iT PicoGreen dsDNA Assay Kit (Invitrogen, Carlsbad, CA, USA) with a Spectra Fluor F129003 (Tecan, Männedorf, Switzerland). The PCR amplicons were pooled in equimolar quantities (110 fmol). The mixed samples were purified and the volume was reduced using a Microcon YM-100 filter (Millipore, Brussels, Belgium). Fragmentation of the products, labeling with biotin, hybridization, washing, and scanning procedures were carried out based on the CustomSeq resequencing array protocol version 2.1 (Affymetrix). An FS450 fluidics station (Affymetrix) was used for washing and staining and a GCS3000 7G scanner (Affymetrix) was used for scanning. To test the efficiency of mutation detection, PCR products containing 20 known heterozygous mutations (Table 3) from three genes (*FBN1*, *TGFBR2*, and *TGFBR1*), as well as another 104 PCR products amplified from normal control DNA, covering all the other exons, were analyzed using the chip. Affymetrix GCOS and GSEQ software were used to process the raw data and analyze the nucleotide sequences, respectively. The default settings of GSEQ were adopted.

Multiplex next-generation sequencing

The PCR amplicons from one patient were mixed and processed using a multiplexing sequencing primers and PhiX control kit (Illumina, San Diego, CA, USA) according to the manufacturer's instructions but with minor changes. In brief, amplicons were fragmented with Covaris S1 (Covaris, Woburn, MA, USA), and purified using Agencourt AMPure (Beckman Coulter, Brea, CA, USA) instead of gel extraction. DNA quality was checked with an Agilent 2100 bioanalyzer (Agilent Technologies, Santa Clara, CA, USA) and a bar code DNA tag (Illumina) was ligated on. The bar code DNA tags contain unique 6 bp sequences and allow the processing of up to 96 DNA fragments in a single run using an Illumina GAIIx (Illumina). Twelve processed DNA fragments, each with a different tag, were mixed and analyzed with single 76 bp reads in one lane of the flow cell. Six lanes were necessary for the analysis of 70 samples. Image analysis and base calling were performed by sequence control software real-time analysis (Illumina) and offline Basecaller software v1.8.0 (Illumina). The reads were aligned to the human reference genome sequence (UCSC hg19, GRCh37) using the ELAND v2 algorithm in CASAVA software v1.7.0 (Illumina).

Table 3 Known mutations used as positive controls for testing ResAT

Nucleotide substitution		Small deletion or insertion	
Gene	Mutation	Gene	Mutation
FBN1	c.400T > G	*FBN1*	c.937delT
	c.772C > T		c.1876delG
	c.1011C > A		c.4283–4284insG
	c.1285C > T		c.7039–7040delAT
	c.2413T > C		
	c.2942G > C		
	c.4099T > C		
	c.4495A > T		
	c.5539T > C		
	c.5788G + 5G > A		
	c.6236C > G		
	c.6773G > A		
TGFBR2	c.1142G > C		
	c.1411G > A		
	c.1624C > T		
TGFBR1	c.1135A > G		

All mutations are previously reported (Sakai et al. 2006; Togashi et al. 2007)

Mapping strategy and variant annotation

An average of 2.4 million reads (ranging from 1.7 to 4.0 million reads) for each sample passed quality control (Path Filter) and were mapped to the human reference genome using mapping and assembly with qualities (MAQ) (Li et al. 2008), NextGENe software v2.00 (SoftGenetics, State College, PA, USA), and Burrows-Wheeler Aligner (BWA)/sequence alignment/map tools (SAMtools) (Li and Durbin 2010; Li et al. 2009). Single nucleotide polymorphisms (SNPs) and indels were extracted from the alignment data using an original script created by BITS, Tokyo, Japan along with information on the registered SNPs (dbSNP131). A consensus quality score of 40 or more was used for the

SNP analysis in MAQ. SNPs in MAQ-passed reads were annotated using the SeattleSeq website (http://gvs.gs.washington.edu/SeattleSeqAnnotation/). A minimum base quality of 13, a minimum root mean square mapping quality for SNPs of 10, and a minimum read depth of 2 were used in BWA/SAMtools (Li and Durbin 2010; Li et al. 2009). NextGENe (SoftGenetics) was also used to analyze the reads, employing default settings apart from using the no-condensation mode. For base substitutions, we focused on variants detected in common by both MAQ and NextGENe. Small indel variants were classified as positive if found by both BWA and NextGENe.

Validation of novel variants

Novel variants (not in dbSNP131, the 1,000 genomes dataset or our in-house database) identified by ResAT and NGS were validated by Sanger sequencing. Surplus PCR products were treated with ExoSAP IT (GE Healthcare, Piscataway, NJ) and sequenced using a standard protocol using BigDye terminators (Applied Biosystems, Foster City, CA, USA) on an ABI PRISM 3100 genetic analyzer (Applied Biosystems). Furthermore, novel variants were screened in 94 Japanese controls by high-resolution melt curve analysis (LightCycler 480; Roche Diagnostics, Basel, Switzerland) and subsequent Sanger sequencing. Novel variants were evaluated using web-based programs including PolyPhen (http://genetics.bwh.harvard.edu/pph/), PolyPhen2 (http://genetics.bwh.harvard.edu/pph2/), Mutation Taster (http://www.mutationtaster.org/), and ESEfinder (http://rulai.cshl.edu/cgi-bin/tools/ESE3/esefinder.cgi?process=home).

Results

Array performance

Across all 70 samples, the mean nucleotide call rate was 95.7% (range 87.3–97.6%) using the default settings of GSEQ. We observed an improvement of the call rate as the number of samples increased. For example, the call rate by GCOS for the first two samples was 90.1 and 90.6% and was 93.3 and 93.9% when 10 samples were analyzed, and was 94.9 and 95.5% when 33 samples were analyzed. However, between 34 and 70 samples, the call rate did not greatly improve (only by 1%). We had constant difficulty in reading approximately 4% of the sequences per array (i.e., no sequence called), mostly in regions of high GC and CC content.

Detection of known mutations by ResAT

To validate the quality of mutation detection in our resequencing array, we analyzed amplicons containing 16 known nucleotide substitutions, three small deletions (1–2 bp), and one 1 bp insertion, plus all the other normal exons (Sakai et al. 2006; Togashi et al. 2007) (Table 3). Fourteen out of 16 nucleotide substitutions were detected (87.5%) by GSEQ in the automated mode. Two mutations (c.772C > T in *FBN1* and c.1142G > C in *TGFBR2*) were not detected. The former was insensitive, and the latter was indicated as a no-call. Visual inspection in the manual mode enabled easy detection of the *TGFBR2* mutation. The mutation detection rate was 93.8% (15/16) using both the automated and manual modes. None of the small indels were detected by our array in either the automated or manual modes.

Variant detection by ResAT

We detected 70 nucleotide substitutions in the automated mode in the 70 patients analyzed (0–3 variants per sample). Fifty-one variants were already registered in dbSNP131 and/or in our in-house database (Supplementary table). The remaining 19 novel variants were validated by Sanger sequencing (Table 4). One variant (c.976–16C > T in *PLOD1*) was homozygous and the others were heterozygous. No indel mutations were detected.

Variant detection by NGS

The target regions were completely covered by NGS reads (100%). The average read depth (coverage of sequence reads) was approximately 600 for each gene (Table 5). The NextGENe software detected a mean of 876 variants in the 70 patients with mutation scores of 10 or more (ranging from 581 to 1209 with SD = 131). MAQ and SeattelSeq detected a mean of 271 variants (ranging from 111 to 384 with SD = 52). Semi-automatic exclusion of variants that were out of the target regions (22 bp or more away from the 5′-end of exons and 9 bp or more away from the 3′-end of exons) or were known variants in dbSNP131 was performed using Excel 2008 for Mac (Microsoft, Redmond, WA, USA), narrowing the data down to 0–6 variants per sample. Twenty novel variants were detected by both MAQ and NextGENe, which were further validated by Sanger sequencing. No indel mutations were detected by MAQ, NextGENe, or BWA/SAMtools.

Comparison of ResAT and NGS variants

Eighteen novel variants were detected by ResAT and NGS. One was detected by ResAT only and two by NGS only. The two variants undetected by ResAT were c.1388G > A (p.Arg463Gln) in *PLOD1* and c.136A > C (p.Ser46Arg) in *TGFBR2*. The former was indicated as a no-call, but was detected later in the manual mode. The latter was within a

Table 4 Novel variants detected by ResAT and/or NGS

Mutation		Amino acid change	Methods of detection	Read depth in NGS	PolyPhen	PolyPhen2	Mutation taster	Patients	Controls (total number)
Gene	Mutation								
TGFBR2	*c.136A > C*[c]	p.Ser46Arg	NGS	472	Benign	Benign (0.099)	Polymorphism	1	0 (94)
	c.403G > T	p.Asp135Tyr	ResAT and NGS	1,257	Possibly damaging	Possibly damaging (0.682)	Polymorphism	1	0 (94)
	c.692C > T[d]	p.Thr231Met	ResAT and NGS	989	Benign	Possibly damaging (0.670)	Polymorphism	1	0 (93)
TGFBR1	*c.1032T > C*	p.Asn344Asn	ResAT and NGS	939	Unknown	–	Polymorphism	1	3 (94)
COL3A1	*c.1815 + 5G > A*		ResAT	255	Unknown	–	Disease-causing	1	0 (94)
	c.84T > C[d]	p.Val28Val	ResAT and NGS	644	Unknown	–	Polymorphism	1	0 (94)
	c.119C > T[e]	p.Ala40Val	ResAT and NGS	1,402	Unknown	Unknown	Polymorphism	1	0 (94)
	c.3133G > A	p.Ala1045Thr	ResAT and NGS	630	Benign	Probably damaging (0.979)	Polymorphism	1	0 (94)
	c.3776C > T	p.Ala1259Val	ResAT and NGS	872	Unknown	Unknown	Disease-causing	1	0 (94)
PLOD1	*c.976–16C > T*[a]		ResAT and NGS	631	unknown	–	polymorphism	1	2[a] (94)
	c.1098–8C > G		ResAT and NGS	633	Unknown	–	Disease-causing	1	0 (94)
	c.1388G > A	p.Arg463Gln	NGS	624, 768	Unknown	Probably damaging (0.961)	Disease-causing	2	4 (94)
	c.1495C > T	p.Arg499Trp	ResAT and NGS	509, 532, 568, 679	Probably damaging	Probably damaging (0.992)	Disease-causing	4	2 (94)
MYH11	*c.4600–13G > A*		ResAT and NGS	1,336	unknown	–	Polymorphism	1	2 (94)
	c.4625G > A[b]	p.Arg1542Gln	ResAT and NGS	1,254	Possibly damaging	Probably damaging (0.994)	Disease-causing	1	0 (94)
	c.4963C > T[b]	p.Arg1655Cys	ResAT and NGS	2,711	Probably damaging	Probably damaging (1.000)	Disease-causing	1	0 (94)
SLC2A10	*c.315C > T*	p.Arg105Arg	ResAT and NGS	543	Unknown	–	Polymorphism	1	0 (94)
	c.330C > T[e]	p.Phe110Phe	ResAT and NGS	500	Unknown	–	Polymorphism	1	0 (94)
	c.1220T > G[b]	p.Leu407Arg	ResAT and NGS	382	Benign	possibly damaging (0.925)	Disease-causing	1	0 (94)
ACTA2	*c.130–18T > C*[c]		ResAT and NGS	607, 647	Unknown	–	Polymorphism	2	2 (94)
	c.482T > C	p.Val161Ala	ResAT and NGS	752	Probably damaging	Beningn (0.013)	Disease-causing	1	0 (94)

The underlined mutation is highly likely to be pathogenic

[a] Homozygous substitution

[b] Mutations detected in patient 16 patient

[c] Mutations detected in patient 24

[d] Mutations detected in patient 28

[e] Mutations detected in patient 89

Table 5 Gene-based read depth in NGS

Gene	Mean depth[a]
FBN1	655
TGFBR2	613
TGFBR1	568
COL3A1	596
PLOD1	607
MYH11	643
SLC2A10	571
ACTA2	543

[a] Based on NextGENe calculation

repetitive sequence. One variant (c.1815 + 5G > A in *COL3A1*) was undetected by NGS due to our set criteria (the variant was detected by MAQ, but not by NextGENe or BWA/SAMtools).

Pathological significance of the variants

We realized that none of the known pathogenic mutations were identified. The pathological impact of the variants was considered if none of the healthy controls showed the same change, if the variants altered evolutionarily conserved amino acids in functional repeats/domains, or if they were predicted to cause abnormal splicing resulting in protein truncation or degradation. Moreover, homozygous and compound heterozygous changes that were found in *PLOD1* and *SLC2A10* may confer autosomal recessive effects. At least three heterozygous variants were considered as putative pathogenic gene alterations (Table 6):

1. c.1815 + 5G > A in *COL3A1* (patient 29). A similar mutation, c.1815 + 5G > T, associated with the skipping of exon 25, was reported in a patient with Ehlers–Danlos syndrome type IV (EDS IV) (Lee et al. 1991b). ESEfinder suggested that the binding position of the splice donor matrix was changed similarly by c.1815 + 5G > A and c.1815 + 5G > T. Thus, C.1815 + 5G > A is highly likely to be pathogenic.
2. c.4963C > T (p.Arg1655Cys) in *MYH11* (patient 16). In addition to this mutation, the patient had two novel heterozygous variants: c.4625G > A (p.Arg1542Gln) in *MYH11* and c.1220T > G (p.Leu407Arg) in *SLC2A10*. Mutations in *SLC2A10* cause autosomal recessive arterial tortuosity syndrome (MIM #208050) (Coucke et al. 2006), although it is unknown whether the heterozygous variant we identified would be related to this, assuming a second-hit model of recessive disease. Both p.Arg 1542Gln and p.Arg1655Cys in *MYH11* were similarly predicted to be pathogenic by three programs (PolyPhen, PolyPhen2, and Mutation Taster). These residues are located in the coiled-coil region, and both are evolutionarily conserved amino acids (Fig. 1). Paircoil2 (http://groups.csail.mit.edu/cb/paircoil2/) was used to predict the effect of variants on the parallel coiled coil fold using pairwise residue probabilities (McDonnell et al. 2006). Paircoil2 indicated that p.Arg1655Cys altered the *p* score from 0.00096 (wild type) to 0.00579 (mutation), while p.Arg1542Gln did not alter the *p* score, 0.00016 (mutation) and 0.00018 (wild type) (Fig. 1). Thus, p.Arg1655Cys was more likely than p.Arg1542Gln to be pathogenic.
3. c.482T > C (p.Val161Ala) in *ACTA2* (patient 27). The patient was found retrospectively to suffer from familial thoracic AAD. The patient has an affected brother, but his DNA was unavailable. Valine at amino acid 161 is evolutionarily conserved and located within the actin domain. However, as we could not analyze the DNA of the affected brother, it may be more appropriate to call this variant 'of unknown significance'.

Discussion

Exon-by-exon Sanger sequencing is the gold standard for genetic analysis, but multiple-gene analysis in many patients is a huge task in terms of time and cost. In this study, we applied two emerging technologies providing rapid and efficient analysis of eight genes in 70 AAD patients. We also compared the results of the two technologies.

The overall mean call rate of our custom array by GSEQ software was 95.7%, which is comparable with previous

Table 6 Pathogenic variants found in the patients

Patient ID	Sex	Mutation	Clinical diagnosis	Age[a]	Age[b]	Family history
Patient 16	M	*MYH11* c.4963C > T p.Arp1655Cys	Thoracic and abdominal AAD	80	80	None
Patient 27	F	*ACTA2* c.482T > C p.Val161Ala	Thoracic AAD	57	46	Affected brother
Patient 29	F	*COL3A1* c.1815 + 5G > A	Thoracic AAD	80	67	None

M male, *F* female

[a] At blood collection

[b] At the first surgery

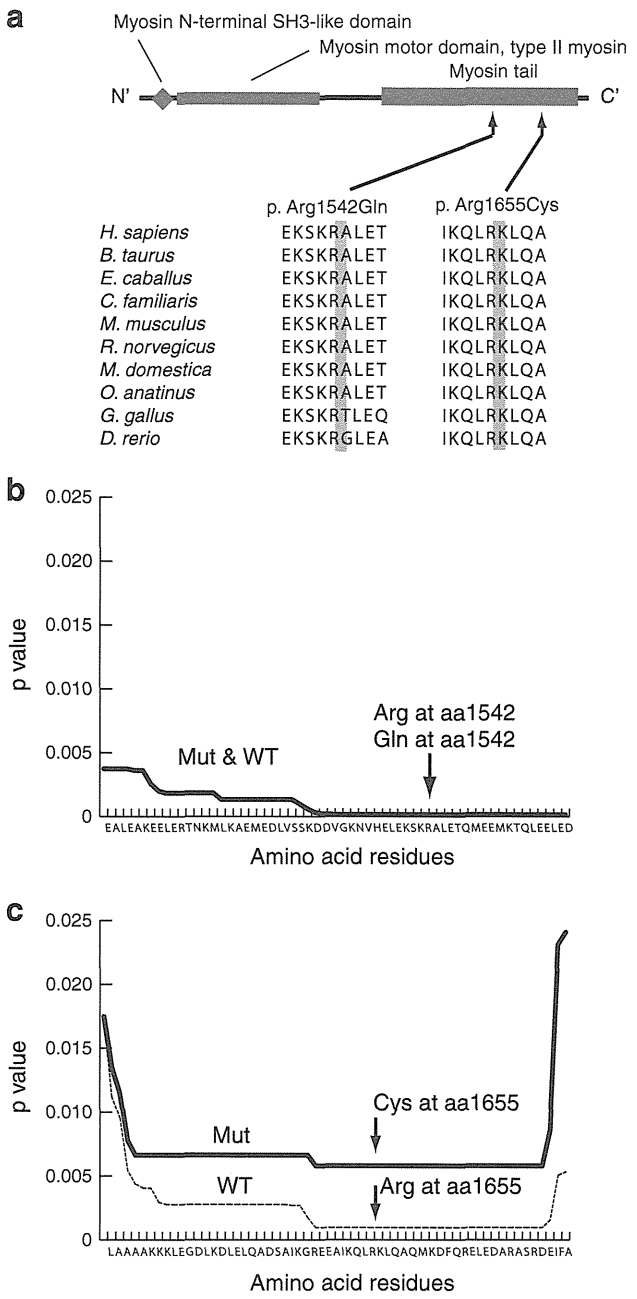

Fig. 1 Double mutations in *MYH11*. **a** Schematic representation of the MYH11 protein. Three functional domains are indicated: the myosin N-terminal SH3-like domain, the myosin motor domain for type II myosin, and the myosin tail. Both the mutations are located in the myosin tail. **b**, **c** Paircoil2 analysis showing a significantly decreased probability of coiled-coil formation for p.Arg1655Cys relative to the wild-type sequence, but no change for p.Arg1542Gln

studies (Bruce et al. 2010; Chiou et al. 2011; Jensen et al. 2011; Schroeder et al. 2010). The call rates became higher as the number of patients increased. Approximately 33 samples were necessary to attain the maximum call-rate in GSEQ. A similar observation was described previously (Fokstuen et al. 2011). No-call regions are one of the problems of ResAT. Other groups have previously suggested that most of the no-call regions are GC- and CC-rich (Bruce et al. 2010; Chiou et al. 2011; Fokstuen et al. 2011). In our custom array, approximately 4% of the target sequences were difficult to obtain (no-calls) in most of the samples.

The mean detection rate of known variants using our custom array and GSEQ with the default settings (automated analysis) was 87.5%. This rate increased to 93.8% after manual inspection. For our ResAT data, the detection rate of nucleotide substitutions in the automated mode was higher, and that in the manual mode was slightly lower, compared with detection rates in previous studies (82.1 vs. 81%, respectively, in automated mode, and 97.4 vs. 100%, respectively, in manual mode) (Bruce et al. 2010; Chiou et al. 2011). Our ResAT analysis was unable to detect any small indel mutations; this is similar to other studies (Hartmann et al. 2009; Kothiyal et al. 2010). In the human gene mutation database (HGMD; http://www.hgmd.cf.ac.uk/ac/index.php), insertions/deletions account for a substantial proportion of the total registered mutations in our genes of interest: *FBN1* 23.6%, *TGFBR2* 6.4%, *TGFBR1* 10%, *COL3A1* 12.8%, *PLOD1* 46.2%, *MYH11* 20%, *SLC2A10* 21.1%, and *ACTA* 20%. Thus, the incapability of ResAT to detect indel mutations is one of its most significant drawbacks.

Our NGS analysis missed one of 21 variants (c.1815 + 5G > A in *COL3A1*). Our protocol focused on variants identified by two different informatics methods, to increase the true-positive rate. For example, MAQ (single-end reads) can detect nucleotide substitutions well, but is not good at detecting small indels (Li et al. 2008). BWA is more sensitive at detecting small indels because it can align gapped sequence (Krawitz et al. 2010). NextGENe is based on the Burrows-Wheeler transform algorithm, which is good at detecting small indels. NGS needs more efficient informatics methods to extract all the nucleotide changes correctly with lower error rates.

In this study, concomitant variants in two genes were detected in four patients (Table 4): c.4625G > A and c.4963C > T in *MYH11*, and c.1220T > G in *SLC2A10* (patient 16); c.136A > C in *TGFBR2* and c.130–18T > C in *ACTA2* (patient 24); c.84T > C in *COL3A1* and c.692C > T in *TGFBR2* (patient 28); c.119C > T in *COL3A1* and c.330C > T in *SLC2A10* (patient 89) (Table 4). It may be quite difficult to detect variants in two or more genes by conventional methods. ResAT and NGS permitted us to find multiple variants in multiple genes easily and rapidly. Double or triple mutations in unusual clinical cases will also be found using such technologies.

Three different putative pathological mutations in a heterozygous state in three of 70 patients were found in this study (4.3%). Interestingly, all the three patients suffered from thoracic AAD. Considering only those patients with

thoracic AAD ($n = 35$), the rate increased to 8.6%. Thus, non-syndromic AAD (especially thoracic AAD) can be explained to some extent by aberrations of genes related to Mendelian disorders, although our sample size was small. Interestingly, among these three patients, only patient 29 showed hyperlipidemia and the other two (patients 16 and 27) did not, which supports the genetic origin of thoracic AAD.

In this study, we compared ResAT and NGS. Considering the drawbacks of ResAT, including its inability to detect small indels and its no-call regions, we believe that NGS is the better technology for comprehensive analysis of multiple genes, especially with improved informatics methods, as it can detect all types of mutations with no bias. Another advantage of NGS is its flexibility. Resequencing array technology requires a custom-made sequencing array. It is not easy or practical to update arrays frequently. However, NGS is currently quite expensive for most laboratories. Next-generation sequencing combined with the pooled genomic DNA method with indexing may improve its cost-effectiveness (Calvo et al. 2010; Druley et al. 2009).

In conclusion, we found that 4.3% of non-syndromic AAD patients (8.5% of thoracic AAD patients) have abnormalities in genes that cause Mendelian disorders. ResAT and NGS enabled multiple genes to be analyzed efficiently. In addition to the 70 AAD patients, a patient with familial Marfan syndrome and a patient with Loeys–Dietz syndrome were initially included before their diagnosis was known. We detected c.6793T > G (p.Cys2265Gly) in *FBN1* in the Marfan syndrome patient [by ResAT (NGS was not done)] and c.797A > G (p.Asp266Gly) in *TGFBR1* in the Loeys–Dietz patient (by ResAT and NGS). We excluded these two patients from this study because they are syndromic AAD patients, but the efficient detection of their mutations highlights the validity of our approach. Finally, high throughput technologies have the potential to routinely identify novel variants of known or unknown significance in clinical settings. Therefore, more sophisticated methods to evaluate gene variants as well as databases containing normal (rare) variants are needed.

Acknowledgments The authors would like to thank the patients for their participation in this study. This work was supported by research grants from the Ministry of Health, Labour and Welfare (N. Matsumoto), the Japanese Science and Technology Agency (N. Matsumoto), the Takeda Science Foundation (N. Matsumoto), the Japanese Prize Foundation (T. Mizuguchi) and a Grant-in-Aid for Scientific Research from the Japanese Society for the Promotion of Science (N. Matsumoto).

References

Bruce CK, Smith M, Rahman F, Liu ZF, McMullan DJ, Ball S, Hartley J, Kroos MA, Heptinstall L, Reuser AJ, Rolfs A, Hendriksz C, Kelly DA, Barrett TG, MacDonald F, Maher ER, Gissen P (2010) Design and validation of a metabolic disorder resequencing microarray (BRUM1). Hum Mutat 31:858–865

Calvo SE, Tucker EJ, Compton AG, Kirby DM, Crawford G, Burtt NP, Rivas M, Guiducci C, Bruno DL, Goldberger OA, Redman MC, Wiltshire E, Wilson CJ, Altshuler D, Gabriel SB, Daly MJ, Thorburn DR, Mootha VK (2010) High-throughput, pooled sequencing identifies mutations in NUBPL and FOXRED1 in human complex I deficiency. Nat Genet 42:851–858

Chiou KR, Charng MJ, Chang HM (2011) Array-based resequencing for mutations causing familial hypercholesterolemia. Atherosclerosis 216(2):383–389

Coucke PJ, Willaert A, Wessels MW, Callewaert B, Zoppi N, De Backer J, Fox JE, Mancini GM, Kambouris M, Gardella R, Facchetti F, Willems PJ, Forsyth R, Dietz HC, Barlati S, Colombi M, Loeys B, De Paepe A (2006) Mutations in the facilitative glucose transporter GLUT10 alter angiogenesis and cause arterial tortuosity syndrome. Nat Genet 38:452–457

Dietz HC, Cutting GR, Pyeritz RE, Maslen CL, Sakai LY, Corson GM, Puffenberger EG, Hamosh A, Nanthakumar EJ, Curristin SM et al (1991) Marfan syndrome caused by a recurrent de novo missense mutation in the fibrillin gene. Nature 352:337–339

Druley TE, Vallania FL, Wegner DJ, Varley KE, Knowles OL, Bonds JA, Robison SW, Doniger SW, Hamvas A, Cole FS, Fay JC, Mitra RD (2009) Quantification of rare allelic variants from pooled genomic DNA. Nat Methods 6:263–265

Farias-Hesson E, Erikson J, Atkins A, Shen P, Davis RW, Scharfe C, Pourmand N (2010) Semi-automated library preparation for high-throughput DNA sequencing platforms. J Biomed Biotechnol 2010:617469

Fokstuen S, Munoz A, Melacini P, Iliceto S, Perrot A, Ozcelik C, Jeanrenaud X, Rieubland C, Farr M, Faber L, Sigwart U, Mach F, Lerch R, Antonarakis SE, Blouin JL (2011) Rapid detection of genetic variants in hypertrophic cardiomyopathy by custom DNA resequencing array in clinical practice. J Med Genet 48(8):572–576

Gabriel C, Danzer M, Hackl C, Kopal G, Hufnagl P, Hofer K, Polin H, Stabentheiner S, Proll J (2009) Rapid high-throughput human leukocyte antigen typing by massively parallel pyrosequencing for high-resolution allele identification. Hum Immunol 70:960–964

Guo DC, Pannu H, Tran-Fadulu V, Papke CL, Yu RK, Avidan N, Bourgeois S, Estrera AL, Safi HJ, Sparks E, Amor D, Ades L, McConnell V, Willoughby CE, Abuelo D, Willing M, Lewis RA, Kim DH, Scherer S, Tung PP, Ahn C, Buja LM, Raman CS, Shete SS, Milewicz DM (2007) Mutations in smooth muscle alpha-actin (ACTA2) lead to thoracic aortic aneurysms and dissections. Nat Genet 39:1488–1493

Hartmann A, Thieme M, Nanduri LK, Stempfl T, Moehle C, Kivisild T, Oefner PJ (2009) Validation of microarray-based resequencing of 93 worldwide mitochondrial genomes. Hum Mutat 30:115–122

Hautala T, Heikkinen J, Kivirikko KI, Myllyla R (1993) A large duplication in the gene for lysyl hydroxylase accounts for the type VI variant of Ehlers–Danlos syndrome in two siblings. Genomics 15:399–404

Jensen LR, Chen W, Moser B, Lipkowitz B, Schroeder C, Musante L, Tzschach A, Kalscheuer VM, Meloni I, Raynaud M, van Esch H, Chelly J, de Brouwer AP, Hackett A, van der Haar S, Henn W, Gecz J, Riess O, Bonin M, Reinhardt R, Ropers HH, Kuss AW (2011) Hybridisation-based resequencing of 17 X-linked intellectual disability genes in 135 patients reveals novel mutations in ATRX, SLC6A8 and PQBP1. Eur J Hum Genet 19(6):717–720

Kothiyal P, Cox S, Ebert J, Husami A, Kenna MA, Greinwald JH, Aronow BJ, Rehm HL (2010) High-throughput detection of mutations responsible for childhood hearing loss using resequencing microarrays. BMC Biotechnol 10:10

Krawitz P, Rodelsperger C, Jager M, Jostins L, Bauer S, Robinson PN (2010) Microindel detection in short-read sequence data. Bioinformatics 26:722–729

Lee B, Godfrey M, Vitale E, Hori H, Mattei MG, Sarfarazi M, Tsipouras P, Ramirez F, Hollister DW (1991a) Linkage of Marfan syndrome and a phenotypically related disorder to two different fibrillin genes. Nature 352:330–334

Lee B, Vitale E, Superti-Furga A, Steinmann B, Ramirez F (1991b) G to T transversion at position +5 of a splice donor site causes skipping of the preceding exon in the type III procollagen transcripts of a patient with Ehlers-Danlos syndrome type IV. J Biol Chem 266:5256–5259

Li H, Durbin R (2010) Fast and accurate long-read alignment with Burrows-Wheeler transform. Bioinformatics 26:589–595

Li H, Ruan J, Durbin R (2008) Mapping short DNA sequencing reads and calling variants using mapping quality scores. Genome Res 18:1851–1858

Li H, Handsaker B, Wysoker A, Fennell T, Ruan J, Homer N, Marth G, Abecasis G, Durbin R (2009) The Sequence Alignment/Map format and SAMtools. Bioinformatics 25:2078–2079

Loeys BL, Chen J, Neptune ER, Judge DP, Podowski M, Holm T, Meyers J, Leitch CC, Katsanis N, Sharifi N, Xu FL, Myers LA, Spevak PJ, Cameron DE, De Backer J, Hellemans J, Chen Y, Davis EC, Webb CL, Kress W, Coucke P, Rifkin DB, De Paepe AM, Dietz HC (2005) A syndrome of altered cardiovascular, craniofacial, neurocognitive and skeletal development caused by mutations in TGFBR1 or TGFBR2. Nat Genet 37:275–281

McDonnell AV, Jiang T, Keating AE, Berger B (2006) Paircoil2: improved prediction of coiled coils from sequence. Bioinformatics 22:356–358

Mizuguchi T, Collod-Beroud G, Akiyama T, Abifadel M, Harada N, Morisaki T, Allard D, Varret M, Claustres M, Morisaki H, Ihara M, Kinoshita A, Yoshiura K, Junien C, Kajii T, Jondeau G, Ohta T, Kishino T, Furukawa Y, Nakamura Y, Niikawa N, Boileau C, Matsumoto N (2004) Heterozygous TGFBR2 mutations in Marfan syndrome. Nat Genet 36:855–860

Ng SB, Bigham AW, Buckingham KJ, Hannibal MC, McMillin MJ, Gildersleeve HI, Beck AE, Tabor HK, Cooper GM, Mefford HC, Lee C, Turner EH, Smith JD, Rieder MJ, Yoshiura K, Matsumoto N, Ohta T, Niikawa N, Nickerson DA, Bamshad MJ, Shendure J (2010) Exome sequencing identifies MLL2 mutations as a cause of Kabuki syndrome. Nat Genet 42:790–793

Sakai H, Visser R, Ikegawa S, Ito E, Numabe H, Watanabe Y, Mikami H, Kondoh T, Kitoh H, Sugiyama R, Okamoto N, Ogata T, Fodde R, Mizuno S, Takamura K, Egashira M, Sasaki N, Watanabe S, Nishimaki S, Takada F, Nagai T, Okada Y, Aoka Y, Yasuda K, Iwasa M, Kogaki S, Harada N, Mizuguchi T, Matsumoto N (2006) Comprehensive genetic analysis of relevant four genes in 49 patients with Marfan syndrome or Marfan-related phenotypes. Am J Med Genet A 140:1719–1725

Schroeder C, Stutzmann F, Weber BH, Riess O, Bonin M (2010) High-throughput resequencing in the diagnosis of BRCA1/2 mutations using oligonucleotide resequencing microarrays. Breast Cancer Res Treat 122:287–297

Superti-Furga A, Gugler E, Gitzelmann R, Steinmann B (1988) Ehlers-Danlos syndrome type IV: a multi-exon deletion in one of the two COL3A1 alleles affecting structure, stability, and processing of type III procollagen. J Biol Chem 263:6226–6232

Togashi Y, Sakoda H, Nishimura A, Matsumoto N, Hiraoka H, Matsuzawa Y (2007) A Japanese family of typical Loeys-Dietz syndrome with a TGFBR2 mutation. Intern Med 46:1995–2000

Tsurusaki Y, Osaka H, Hamanoue H, Shimbo H, Tsuji M, Doi H, Saitsu H, Matsumoto N, Miyake N (2011) Rapid detection of a mutation causing X-linked leucoencephalopathy by exome sequencing. J Med Genet 48(9):606–609

Wang L, Guo DC, Cao J, Gong L, Kamm KE, Regalado E, Li L, Shete S, He WQ, Zhu MS, Offermanns S, Gilchrist D, Elefteriades J, Stull JT, Milewicz DM (2010) Mutations in myosin light chain kinase cause familial aortic dissections. Am J Hum Genet 87:701–707

Zhu L, Vranckx R, Khau Van Kien P, Lalande A, Boisset N, Mathieu F, Wegman M, Glancy L, Gasc JM, Brunotte F, Bruneval P, Wolf JE, Michel JB, Jeunemaitre X (2006) Mutations in myosin heavy chain 11 cause a syndrome associating thoracic aortic aneurysm/aortic dissection and patent ductus arteriosus. Nat Genet 38:343–349

Zimmerman RS, Cox S, Lakdawala NK, Cirino A, Mancini-DiNardo D, Clark E, Leon A, Duffy E, White E, Baxter S, Alaamery M, Farwell L, Weiss S, Seidman CE, Seidman JG, Ho CY, Rehm HL, Funke BH (2010) A novel custom resequencing array for dilated cardiomyopathy. Genet Med 12:268–278

PLOS ONE

Common and Distinct Clinical Features in Adult Patients with Anti-Aminoacyl-tRNA Synthetase Antibodies: Heterogeneity within the Syndrome

Yasuhito Hamaguchi[1], Manabu Fujimoto[1]*, Takashi Matsushita[1], Kenzo Kaji[1], Kazuhiro Komura[1], Minoru Hasegawa[1], Masanari Kodera[2], Eiji Muroi[3], Keita Fujikawa[4], Mariko Seishima[5], Hidehiro Yamada[6], Ryo Yamada[7], Shinichi Sato[8], Kazuhiko Takehara[1], Masataka Kuwana[9]

1 Department of Dermatology, Kanazawa University Graduate School of Medical Science, Kanazawa, Japan, **2** Department of Dermatology, Social Insurance Chukyo Hospital, Nagoya, Japan, **3** Department of Dermatology, Nagasaki University Graduate School of Biomedical Sciences, Nagasaki, Japan, **4** Unit of Translational Medicine, Department of Immunology and Rheumatology, Nagasaki University Graduate School of Biomedical Sciences, Nagasaki, Japan, **5** Department of Dermatology, Ogaki Municipal Hospital, Ogaki, Japan, **6** Division of Rheumatology, Department of Internal Medicine, and Allergy, St. Marianna University, Kawasaki, Japan, **7** Center for Genomic Medicine, Graduate School of Medicine, Kyoto University, Kyoto, Japan, **8** Department of Dermatology, Faculty of Medicine, University of Tokyo, Tokyo, Japan, **9** Division of Rheumatology, Department of Internal Medicine, Keio University School of Medicine, Tokyo, Japan

Abstract

Objective: To identify similarities and differences in the clinical features of adult Japanese patients with individual anti-aminoacyl-tRNA synthetase antibodies (anti-ARS Abs).

Methods: This was a retrospective analysis of 166 adult Japanese patients with anti-ARS Abs detected by immunoprecipitation assays. These patients had visited Kanazawa University Hospital or collaborating medical centers from 2003 to 2009.

Results: Anti-ARS Ab specificity included anti-Jo-1 (36%), anti-EJ (23%), anti-PL-7 (18%), anti-PL-12 (11%), anti-KS (8%), and anti-OJ (5%). These anti-ARS Abs were mutually exclusive, except for one serum Ab that had both anti-PL-7 and PL-12 reactivity. Myositis was closely associated with anti-Jo-1, anti-EJ, and anti-PL-7, while interstitial lung disease (ILD) was correlated with all 6 anti-ARS Abs. Dermatomyositis (DM)-specific skin manifestations (heliotrope rash and Gottron's sign) were frequently observed in patients with anti-Jo-1, anti-EJ, anti-PL-7, and anti-PL-12. Therefore, most clinical diagnoses were polymyositis or DM for anti-Jo-1, anti-EJ, and anti-PL-7; clinically amyopathic DM or ILD for anti-PL-12; and ILD for anti-KS and anti-OJ. Patients with anti-Jo-1, anti-EJ, and anti-PL-7 developed myositis later if they had ILD alone at the time of disease onset, and most patients with anti-ARS Abs eventually developed ILD if they did not have ILD at disease onset.

Conclusion: Patients with anti-ARS Abs are relatively homogeneous. However, the distribution and timing of myositis, ILD, and rashes differ among patients with individual anti-ARS Abs. Thus, identification of individual anti-ARS Abs is beneficial to define this rather homogeneous subset and to predict clinical outcomes within the "anti-synthetase syndrome."

Citation: Hamaguchi Y, Fujimoto M, Matsushita T, Kaji K, Komura K, et al. (2013) Common and Distinct Clinical Features in Adult Patients with Anti-Aminoacyl-tRNA Synthetase Antibodies: Heterogeneity within the Syndrome. PLoS ONE 8(4): e60442. doi:10.1371/journal.pone.0060442

Editor: Frederick Miller, National Institutes of Health, United States of America

Received November 13, 2012; **Accepted** February 27, 2013; **Published** April 3, 2013

Funding: This work was supported by a research grant on intractable diseases from the Ministry of Health, Labor and Welfare of Japan (to Manabu Fujimoto). The funders had no role in study design, data collection and analysis, decision to publish, or preparation of the manuscript.

Competing Interests: The authors have declared that no competing interests exist.

* E-mail: fujimoto-m@umin.ac.jp

Introduction

The presence of autoantibodies (Abs) is one of the hallmarks of connective tissue diseases, such as systemic lupus erythematosus (SLE), systemic sclerosis (SSc), and idiopathic inflammatory myopathy. In particular, a variety of serum Abs is found in patients with idiopathic inflammatory myopathies, including polymyositis (PM) and dermatomyositis (DM) [1,2]. It is clinically of considerable importance to identify Abs in patients with PM/DM, because each Ab is closely associated with certain clinical features [3]. For example, anti-Mi-2 is associated with classic DM without interstitial lung disease (ILD) or malignancy and with good response to treatment [4–6]; anti-155/140 is associated with malignancy-associated or juvenile DM [7–10]; and anti-CADM-140/MDA5 is associated with clinically amyopathic DM (CADM) and rapidly progressive-ILD (RP-ILD) that results in poor prognosis [11,12]. Abs reactive with aminoacyl-tRNA synthetases (ARS) are also representative Abs that are detected in patients with PM/DM. Eight anti-ARS Abs have been described: anti-histidyl (anti-Jo-1), anti-threonyl (anti-PL-7), anti-alanyl (anti-PL-12), anti-glycyl (anti-EJ), anti-isoleucyl (anti-OJ), anti-asparaginyl (anti-KS), anti-phenylalanyl (anti-Zo), and anti-tyrosyl (anti-Ha) tRNAs [13–20]. Based on a unique combination of clinical features commonly observed in patients with anti-ARS Abs, Targoff proposed a

disease entity termed "anti-synthetase syndrome," which is characterized by myositis, ILD, fever, Raynaud's phenomenon, arthritis, and mechanic's hands [21]. Although anti-synthetase syndrome has common clinical manifestations, further observations have distinguished some differences in clinical features associated with individual anti-ARS Abs [22]. For example, it has been reported that anti-Jo-1 Abs are closely associated with myositis [14,17], whereas patients with anti-KS are more likely to have ILD without clinical evidence of myositis [18,23]. On the other hand, Sato *et al* previously reported that the presence of anti-PL-7 is closely associated with PM/DM-SSc overlap as well as ILD in Japanese patients [24].

This is a large comprehensive study to focus on the clinical and laboratory features in adult patients with anti-ARS Abs for the investigation of similarities and differences in these anti-ARS Abs. The results of this study indicate that anti-ARS Abs share several clinical features, but also have some considerable differences. Thus, identification of each anti-ARS Ab is beneficial to define this rather homogeneous subset of patients and to predict clinical outcomes.

Patients and Methods

Ethics Statement

Ethical approval for the study was obtained from the individual institutional review boards (Kanazawa University, Keio University, Nagasaki University, St. Marianna University, Social Insurance Chukyo Hospital, and Ogaki Municipal Hospital) and all sera were collected after the subjects gave their written informed consent.

Patients and Sera

Serum samples were obtained from Japanese patients with autoimmune diseases or related disorders who had visited Kanazawa University Hospital or collaborating medical centers from 2003 to 2009. In total, 3164 samples (from 478 patients with DM/PM, 498 with SSc, 183 with ILD alone, 376 with SLE, 102 with mixed connective tissue disease, 398 with Sjogren's syndrome, and 1129 with rheumatoid arthritis) were screened by immunoprecipitation (IP) assay for the detection of antinuclear or anticytoplasmic antibodies. These patients were referred mainly by rheumatologists, dermatologists, or pulmonologists. PM and classic DM were defined by fulfillment of the Bohan and Peter criteria for definite or probable diagnoses [25]. DM was distinguished from PM based on the presence of heliotrope rash or Gottron's lesions (Gottron's papules and/or Gottron's sign). The diagnosis of CADM was based on the criteria proposed by Sontheimer [26], as follows: clinical skin manifestations typical of DM but minimal or no clinical features of myositis for >2 years after the onset of skin manifestations. All patients with SLE or SSc fulfilled the American College of Rheumatology criteria [27,28]. PM/DM-overlap was diagnosed by the coexistence of SLE and/or SSc in addition to PM or DM. "ILD alone" was defined by the presence of ILD without fulfillment of any of the criteria for PM, DM, CADM, SLE, or SSc. Patients with ILD alone were examined for potential coexistence of myositis by evaluating muscle weakness and serum muscle enzyme levels including creatine kinase (CK) and aldolase during follow-up, while those without ILD were examined for potential coexistence of ILD by examining dyspneic symptoms and chest radiograph and/or high-resolution computed tomography (HRCT) at every 3 to 6 months.

Clinical information was collected retrospectively for all patients with anti-ARS Abs by reviewing their clinical charts. Initial manifestations were defined as the clinical presentation at the first clinic visit. Patients who had at least one of the following symptoms: symmetrical proximal muscle weakness, muscle pain, or elevated levels of myogenic enzymes, underwent electromyogram, MRI, and/or muscle biopsy for confirmation of the presence of myositis. Patients were diagnosed with myositis if at least one of these confirmatory examinations showed findings compatible with inflammatory myopathy: a myogenic pattern on electromyogram [25], muscular edema on T2-weighted images with fat suppression on MRI [29], or necrosis, regeneration, and some atrophy of muscle fibers and inflammatory cell infiltration on muscle biopsy [25]. Patients were diagnosed as having ILD according to the images on chest HRCT. RP-ILD was defined as progressive dyspnea and progressive hypoxemia with a worsening of interstitial changes on the chest images within 1 month from the onset of respiratory manifestations [11]. Internal and hematologic malignancies in anti-ARS-positive patients was defined if the malignant disease was diagnosed concurrently with or within 3 years after diagnosis of anti-synthetase syndrome or if a preceding malignant disease occurred within 3 years before diagnosis of anti-synthetase syndrome [4]. Sjögren's syndrome was defined in accordance with the revised European criteria [30].

IP Assays

Protein IP assays were carried out with extracts of the leukemia cell line, K562 [11]. A total of 10 µl of the patient's serum was bound to 2 mg protein-A Sepharose beads (Amersham Biosciences, Piscataway, NJ) in 500 µl of IP buffer (10 mM Tris-HCl, pH 8.0, 50 mM NaCl, 0.1% Nonidet P-40), incubated for 2 h at 4°C, and then washed five times with IP buffer. Ab-coated Sepharose beads were mixed with 100 µl ^{35}S-methionine-labelled K562 cell extracts derived from 10^6 cells and rotated at 4°C for 2 h. After five washes, the beads were resuspended in sodium dodecyl sulphate (SDS) sample buffer and the polypeptides were fractionated by 7.5% SDS-polyacrylamide gel electrophoresis (PAGE) followed by autoradiography. For the analysis of RNA, immunoprecipitated RNA was detected in 8% urea-PAGE from a cell extract obtained from 3×10^6 non-radiolabeled K562 cells by phenol/chloroform, visualized by silver staining [31]. Each anti-ARS Ab was considered positive if serum samples produced precipitin lines with immunological identity to reference sera by both protein and RNA IP [32]. Anti-Ro Ab and anti-La Ab were detected by IP assays as well. Serum was considered positive for anti-Ro Ab if at least one of the Y1–Y5 RNAs was detected by RNA IP and the 60 kDa protein was detected by protein IP; serum was considered positive for anti-La Ab if RNAs contained in the 7S and 5.8S lesions were detected by RNA IP and the 48 kDa protein was detected by protein IP.

Immunofluorescence

Indirect immunofluorescence tests were carried out with slides of monolayer HEp-2 cells (Medical & Biological Laboratories [MBL], Nagoya, Japan) as substrate [33]. Anticentromere antibody was considered positive if serum diluted at 1:40 produced a characteristic staining pattern on HEp-2 cells as well as on commercially prepared HeLa cell chromosomal spreads (MBL) [34].

Statistical Analysis

Frequencies among all six anti-ARS-positive subgroups were compared with a chi-square test. If the overall P value was less than 0.05, pairwise comparisons were performed with a chi-square test with Yates' correction where appropriate. Continuous variables confirmed to be normally distributed were shown as mean and SD, and their comparisons among groups were carried

out with an ANOVA. All statistical analyses were performed with StatView software.

Results

Detection of Anti-ARS Abs

Of 3164 samples screened by IP assays, anti-ARS Abs were detected in 166 patients (5.2%) (Figure 1). As shown in Figure 2, 6 anti-ARS specificities, including anti-Jo-1, anti-EJ, anti-PL-7, anti-PL-12, anti-KS, anti-OJ, were easily detectable and distinguishable by IP assays. Of 166 patients with anti-ARS Abs, anti-Jo-1 was found in 59 (36%) patients, anti-EJ was found in 38 (23%) patients, anti-PL-7 was found in 30 (18%) patients, anti-PL-12 was found in 19 (11%) patients, anti-KS was found in 13 (8%) patients, and anti-OJ was found in 8 (5%) patients. One patient with classic DM had antibodies reactive to both PL-7 and PL-12, and was excluded from the following analyses for clinical associations.

Coexistence of anti-ARS Abs and other autoimmune connective tissue disease-related Abs was examined (Table 1). Antibodies against Mi-2, 155/140, CADM-140/MDA5, MJ/NXP-2, topoisomerase I, centromere, U1RNP, Th/To, U3RNP, Sm and La/SS-B were rarely found in patients with anti-ARS Abs. In contrast, anti-Ro/SS-A Abs were found in 31 (19%) patients. These results were principally consistent with previous findings that myositis-specific Abs are relatively mutually exclusive, while myositis-associated Abs coexist with myositis-specific Abs [13,35].

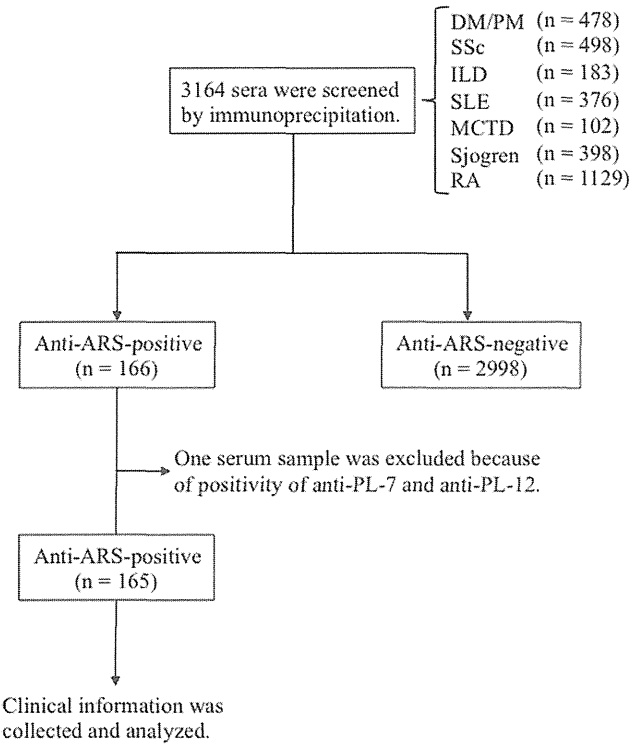

Figure 1. Enrollment and selection of patients. DM; dermatomyositis, PM; polymyositis, SSc; systemic sclerosis, ILD; interstitial lung disease, SLE; systemic lupus erythematosus, MCTD; mixed connective tissue disease, Sjogren; Sjogren's syndrome, RA; rheumatoid arthritis.
doi:10.1371/journal.pone.0060442.g001

Associations between Clinical Diagnoses and Anti-ARS Abs

The distributions of classic DM, CADM, PM, PM/DM-overlap, SLE, SSc, and ILD alone in patients with individual anti-ARS Abs are shown in Figure 3. More than half of the patients with anti-Jo-1, anti-EJ, or anti-PL-7 had apparent myositis, including classic DM, PM, and PM/DM-overlap. The proportion with ILD alone was different among patients with various anti-ARS Abs. In particular, 10 of 13 (77%) patients with anti-KS and 5 of 8 (63%) patients with anti-OJ were diagnosed with ILD alone. Some patients with anti-ARS Abs were diagnosed with SSc or SLE, but the frequency was relatively low. Thus, most patients with anti-ARS Abs were diagnosed as having classic DM, CADM, PM, PM/DM-overlap, or ILD alone, while the proportion of these diagnoses was different among the subgroups of each anti-ARS Ab.

Comparison of Clinical Features among Patients with Anti-ARS Abs

A total of 95 patients with anti-ARS Abs had myositis and were diagnosed as having classic DM, PM, or PM/DM-overlap. We first compared clinical features between patients with myositis in the presence and absence of anti-ARS Ab (n = 95 and 152, respectively). Anti-ARS-positive patients with myositis had higher frequencies of Raynaud's phenomenon ($P = 0.034$), ILD ($P < 0.0001$), and polyarthritis ($P = 0.0015$) compared with anti-ARS-negative patients with myositis. There was no difference in the frequency of fever between the two groups ($P = 0.87$).

Then, we compared the demographic features among anti-ARS-based subgroups, as shown in Table 2. No differences were found in age of onset or sex. We next compared muscle weakness and ILD among individual anti-ARS subgroups, both at the initial visit and during the entire follow-up period. Muscle weakness was found in 71 (43%) patients at the initial visit and 95 (58%) during the entire follow-up period, but the frequencies varied among anti-ARS-based subgroups (overall $P = 0.0011$ and $P < 0.0001$, respectively). Patients with anti-Jo-1, anti-EJ, and anti-PL-7 had a higher frequency of muscle weakness (59%, 39%, and 52%, respectively, at the initial visit and 78%, 55%, and 76%, respectively during the entire follow-up period) than those with anti-PL-12 (17% for both), anti-KS (7% for both), and anti-OJ (25% for both). In contrast, most patients had ILD at the initial visit, and almost all patients eventually suffered from ILD. While most of them had the chronic type of ILD, a total of 13 patients (8 with anti-Jo-1, 4 with anti-EJ, and 1 with anti-PL-7) developed RP-ILD at their first visit or during their clinical course. Thus, the frequency of muscle weakness varied among anti-ARS subgroups, while ILD was observed at equally high frequencies among these subgroups.

Fever, Raynaud's phenomenon, polyarthritis, and mechanic's hands during the entire follow-up period were compared among anti-ARS subgroups. The frequency of fever varied among anti-ARS-based subgroups (8–44%), but there was no statistical difference. Raynaud's phenomenon was found in 40 of 165 (24%) patients with anti-ARS Abs and more frequently observed in patients with anti-PL-12 and anti-PL-7 (overall $P = 0.044$). Polyarthritis was most common in patients with anti-Jo-1 (58%) and infrequently observed in patients with anti-OJ (13%) (overall $P = 0.0029$). Mechanic's hands, which are the representative skin manifestation in anti-synthetase syndrome, were observed in all anti-ARS Ab-based subgroups, but the frequency was highest in patients with anti-Jo-1 (56%) (overall $P = 0.031$). Collectively, Raynaud's phenomenon, polyarthritis, and mechanic's hands were

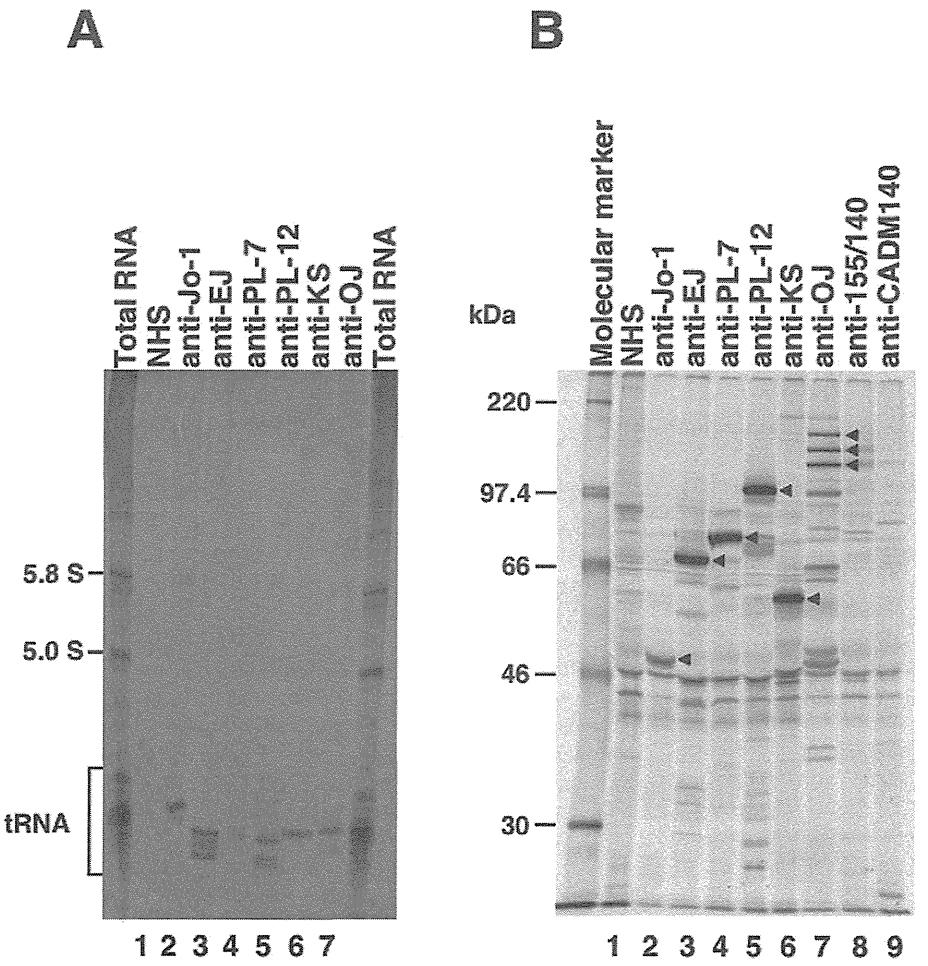

Figure 2. Representative immunoprecipitation assay for RNA with anti-aminoacyl-tRNA synthetase (anti-ARS) sera. A, Immunoprecipitation of histidyl-tRNA synthetase, glycyl-tRNA synthetase, threonyl-tRNA synthetase, alanyl-tRNA synthetase, asparaginyl-tRNA, and isoleucyl-tRNA synthetase by sera. K562 cell extracts were immunoprecipitated with sera, and RNA was extracted, electrophoresed on 8% urea-polyacrylamide gels, and visualized by silver staining. Total RNA, with the 5.8 and 5.0 S small ribosomal RNAs and the tRNA region indicated; Lane 1, normal health serum (NHS) indicated; Lanes 2–7: anti-ARS sera indicated, with antibodies to Jo-1 (histidyl-tRNA synthetase), EJ (glycyl-tRNA synthetase), PL-7 (threonyl-tRNA synthetase), PL-12 (alanyl-tRNA synthetase), KS (asparaginyl-tRNA synthetase), and OJ (isoleucyl-tRNA synthetase). **B,** Immunoprecipitation of ^{35}S-methionine-labeled K562 cell extracts was performed on anti-ARS sera and NHS, separated on 10% SDS-PAGE, and analyzed by autoradiography. Molecular weight markers include protein bands corresponding to 220, 97.4, 66, 46, and 30 kDa.
doi:10.1371/journal.pone.0060442.g002

observed in each anti-ARS Ab subgroup, but the frequencies were rather heterogeneous.

We then compared heliotrope rash and Gottron's signs, which are the representative skin manifestations in DM. Heliotrope rash was found in 26 of 165 (16%) patients with anti-ARS Abs (overall $P = 0.0019$) and Gottron's sign (elbow and/or knee) was found in 51 (31%) (overall $P = 0.043$). These manifestations were predominantly found in patients with anti-EJ, anti-PL-7, and anti-PL-12.

With regard to laboratory findings, CK levels were lower in patients with anti-PL-12 and anti-KS (overall $P = 0.024$), and lactate dehydrogenase (LDH) was lowest in patients with anti-KS (overall $P = 0.019$). It is likely that these results were associated with the frequencies of muscle involvement. KL-6 and pulmonary surfactant protein D (SP-D) levels are associated with the activity and severity of ILD [36,37]. While elevations of both KL-6 and SP-D were observed in all anti-ARS-based subgroups, no significant differences were observed in serum KL-6 and SP-D levels.

As an association of malignancy with PM/DM has been reported, we examined the frequency of malignancies in patients with anti-ARS Abs (Table 2). Malignancies were observed in 19 (12%) of 165 patients with anti-ARS Abs, and 1 of those had a double malignancy. A summary of the malignancies is listed in Table 3. There were 4 patients with colon cancer, 4 with gastric cancer or carcinoid, 3 with breast cancer, 3 with lung cancer, and single cases of prostate cancer, nasopharyngeal cancer, uterine corpus cancer, thyroid cancer, ovarian cancer, and non-Hodgkin lymphoma. There was no trend in the prevalence of malignancy or the type of malignancy among anti-ARS-based subgroups. Seven of 19 patients with malignancy simultaneously developed PM/DM or ILD, while 7 of 19 had malignancy prior to the development of PM/DM or ILD, and 5 of 19 developed malignancy after the diagnosis of PM/DM or ILD.

Table 1. Coexistence of other autoantibodies in patients with anti-aminoacyl-tRNA synthetase antibodies.*

	Anti-Jo-1 (n = 59)	Anti-EJ (n = 38)	Anti-PL-7 (n = 29)	Anti-PL-12 (n = 18)	Anti-KS (n = 13)	Anti-OJ (n = 8)	Anti-PL-7/ PL-12 (n = 1)
Anti-Mi-2	0	0	0	0	0	0	0
Anti-155/140	0	0	0	0	0	0	0
Anti-CADM-140/MDA5	0	0	0	0	0	0	0
Anti-MJ/NXP-2	0	0	0	0	0	0	0
Anti-topoisomerase I	0	1	0	0	0	0	0
Anti-centromere	1	0	0	1	2	0	0
Anti-U1RNP	0	0	1	1	0	0	0
Anti-Th/To	0	0	0	1	0	0	0
Anti-U3RNP	1	0	0	0	0	0	0
Anti-Sm	0	0	1	0	0	0	0
Anti-Ro/SS-A	9	9	8	4	1	0	0
Anti-La/SS-B	0	2	2	0	0	0	0

*Values are the number of patients.
doi:10.1371/journal.pone.0060442.t001

Causes of Death

Sixteen (10%) of 165 anti-ARS-positive patients died during the follow-up period (Table 4). Causes of death included ILD in 8, malignancy in 3, infection in 2, and one each of myocardial infarction, rupture of an abdominal aortic aneurysm, and hypertrophic cardiomyopathy.

Timing of Development of ILD and Myositis in Patients with Anti-ARS Abs

Initial manifestations in patients with anti-ARS Abs are summarized in Table 5. At initial presentation, the combination of manifestations, including DM rashes, myositis, and ILD, varied among patients with anti-ARS Abs. The frequency of ILD alone at

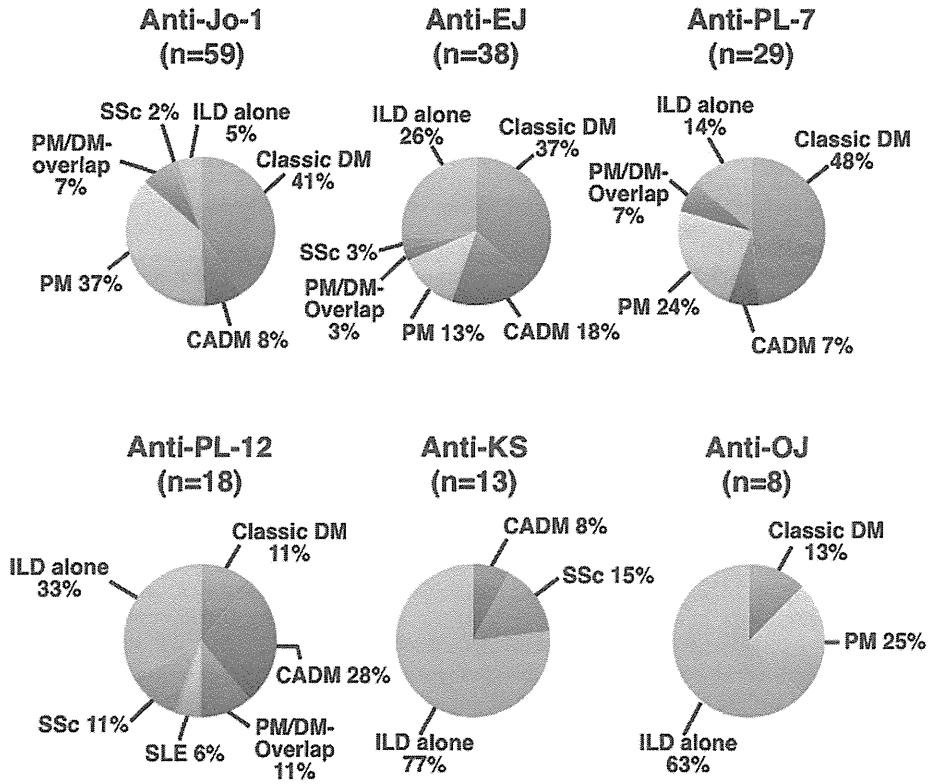

Figure 3. Prevalence of dermatomysitis (DM), clinically amyopathic DM (CADM), polymyositis (PM), PM/DM-overlap, systemic lupus erythematosus (SLE), systemic sclerosis (SSc), and interstitial lung disease (ILD) alone, in each subgroup of anti-synthetase syndrome.
doi:10.1371/journal.pone.0060442.g003

Table 2. Comparison of clinical features in 165 adult Japanese patients with anti-aminoacyl-tRNA synthetase antibodies.*

	Anti-Jo-1 (n = 59)	Anti-EJ (n = 38)	Anti-PL-7 (n = 29)	Anti-PL-12 (n = 18)	Anti-KS (n = 13)	Anti-OJ (n = 8)	Overall *P*
Age at onset, median (range), y	53 (22–76)	53 (18–78)	53 (25–79)	48 (20–75)	54 (39–67)	57 (32–79)	0.61
No. of females/no. of males	43/16	32/6	26/3	16/2	7/6	6/2	0.077
Clinical features (at initial visit)							
Interstitial lung disease	71	84	76	89	100	100	0.077
Muscle weakness	59	39	52	17	7	25	0.0011[a]
Clinical features (entire follow-up period)							
Fever	27	39	34	44	8	13	0.16
Raynaud's phenomenon	19	13	38	44	31	13	0.044[b]
Interstitial lung disease	90	97	93	94	100	100	0.56
Muscle weakness	78	55	76	17	7	25	<0.0001[c]
Polyarthritis	58	24	31	22	31	13	0.0029[d]
Erosive arthritis	12	5	0	17	23	0	0.16
Malignancy	15	3	7	17	15	25	0.22
Sjögren's syndrome	7	16	14	0	8	0	0.32
Skin manifestations							
Heliotrope rash	7	21	38	17	0	0	0.0019[e]
Gottron's sign (hand)	44	45	41	33	8	13	0.10
Gottron's sign (elbow and/or knee)	27	39	45	33	0	13	0.043[f]
Mechanic's hands	56	29	45	22	23	38	0.031[g]
Laboratory findings							
CK, IU/L, mean ± SD	2213±3168	1681±2967	1768±2096	250±306	143±84	881±1129	0.024[h]
LDH, IU/L, mean ± SD	595±5961	427±223	565±406	346±187	215±77	355±197	0.019[i]
KL-6, U/mL, mean ± SD	1335±2067 (n = 54)	1425±1030	1374±1444	1630±1650	1527±1404 (n = 12)	1307±877	0.99
SP-D, ng/mL, mean ± SD	206±229 (n = 39)	318±626 (n = 36)	229±275 (n = 25)	250±170 (n = 15)	185±129	123±53 (n = 6)	0.74

*Unless noted otherwise, values are percentages of patients. NS: not significant; CK: creatine kinase; LDH: lactate dehydrogenase. One patient with DM who had antibodies reactive to both PL-7 and PL-12 was excluded from the analysis. Significant differences (overall $P<0.05$) were further analyzed by pairwise comparisons.
[a]$P<0.05$ between anti-PL-7 and anti-PL-12; $P<0.01$ between anti-Jo-1 and anti-PL-12, and between anti-KS and anti-Jo-1 or anti-PL-7;
[b]$P<0.05$ between anti-Jo-1 and anti-PL-7 or anti-PL-12, and between anti-EJ and anti-PL-7; $P<0.01$ between anti-EJ and anti-PL-12.
[c]$P<0.05$ between anti-EJ and anti-PL-12; $P<0.01$ between anti-Jo-1 and anti-PL-12, anti-KS or anti-OJ, between anti-EJ and anti-KS, and between anti-PL-7 and anti-PL-12, anti-KS or anti-OJ.
[d]$P<0.05$ between anti-Jo-1 and anti-PL-7, anti-KS or anti-OJ; $P<0.01$ between anti-Jo-1 and anti-EJ or anti-PL-12.
[e]$P<0.05$ between anti-Jo-1 and anti-EJ; $P<0.01$ between anti-PL-7 and anti-Jo-1 or anti-KS.
[f]$P<0.05$ between anti-KS and anti-EJ or anti-PL-12; $P<0.01$ between anti-PL-7 and anti-KS.
[g]$P<0.05$ between anti-Jo-1 and anti-PL-12 or anti-KS; $P<0.01$ between anti-Jo-1 and anti-EJ.
[h]$P<0.05$ between anti-EJ and anti-PL-12 or anti-KS; $P<0.01$ between anti-Jo-1 and anti-PL-12 or anti-KS, and between anti-PL-7 and anti-PL-12 or anti-KS.
[i]$P<0.05$ between anti-PL-7 and anti-PL-12; $P<0.01$ between anti-Jo-1 and anti-PL-12, and between anti-KS and anti-Jo-1, anti-EJ or anti-PL-7.
doi:10.1371/journal.pone.0060442.t002

presentation was different among groups stratified by anti-ARS Abs (overall $P=0.0001$). While some patients with anti-ARS Abs had 2 or more manifestations at initial diagnosis, others sequentially developed different manifestations, even when they were receiving therapy. Thus, we analyzed the timing of development of ILD and myositis. Figure 4A includes patients with ILD alone and DM rashes and ILD, and Figure 4B includes those with myositis alone and DM rashes and myositis at initial presentation. Patients with DM rashes alone, myositis and ILD, DM rashes, myositis, and ILD, and none of DM rashes, myositis, and ILD were excluded from this analysis. We assessed whether patients who had ILD alone at presentation developed myositis during follow-up (Figure 4A). As a result, 39%, 29%, and 64% of patients with anti-Jo-1, anti-EJ, and anti-PL-7, respectively, subsequently developed myositis. In contrast, none of the patients with anti-PL-12, anti-KS, and anti-OJ who had ILD alone at presentation developed myositis later in the course of the disease. The distribution of the frequencies for developing myositis among anti-ARS-based subgroups was statistically significant (overall $P=0.0008$). In contrast, when patients who had myositis without ILD at presentation were selected, nearly all of them developed ILD later in the course of the disease (Figure 4B). There was no difference in observation period among the 6 groups (Jo-1, 62±24; EJ, 56±27; PL-7, 50±27; PL-12, 53±27; KS, 70±20; and OJ, 62±32 months). In addition, there was no difference in initial treatment regimen among the 6 groups stratified by anti-ARS Abs (Table 6), although 38% of patients with anti-KS did not receive immunosuppressive therapy and this frequency was highest among the 6 groups (overall $P=0.0070$). Almost all patients with anti-ARS Abs who had ILD or myositis received immunosuppressive treatment, including corticosteroids alone or in combination with immunosuppressants. Accordingly, patients with anti-PL-12, anti-